Evo-Devo Researches on the Novelties of Molluscs

A Dissertation Submitted to

the Graduate School of Life and Environmental Sciences,

the University of Tsukuba

in Partial Fulfillment of the Requirements

for the Degree of Doctor of Philosophy in Science

(Doctoral Program in Biological Science)

Naoki HASHIMOTO

Table of Contents

Abstract

The organisms acquired evolutionarily new characters which are never seen in other lineages. Such novel characters are important for survival and adaptation. However, the origin and evolutionary causes for novelty is still unknown in many structures. In this thesis, I investigated the evolutionary mechanisms for acquisition of novelties by focusing on two novel structures of molluscs, the operculum and two shell plates. The operculum is one of the novelties in gastropods. Because the operculum shows notable similarities to shell, I asked whether there were evolutionary link between these two secretory structures by molecular developmental approaches. I found some of the genes which are expressed in shell glands were also expressed in operculum glands. Moreover, RNAi experiment showed the dpp homolog, *Nf-dpp*, had critical roles for development of both structures. Based on these observations, I suggest that co-option of *dpp* signaling pathway contributed to the innovation of the operculum in gastropods. Bivalves have two shell plates and they are thought to have evolved from single shelled ancestor. Because it is thought that modification of cleavage pattern involved this evolutionary event, I researched regulatory mechanism of cleavage pattern in bivalves. I performed cell isolation experiments to determine whether the unique cleavage pattern of X

blastomere is regulated depending on the interaction with other cells or by cell autonomous mechanism. When focusing on the largest derivatives of D blastomeres, isolated D blastomeres followed the cleavage pattern of normal development up to bilateral cleavage. This result suggests that D blastomeres control their unique cleavage pattern including the reversions of the cell size polarity through intrinsic mechanisms.

General Introduction

Although development of all animals starts from simple spherical form, an egg, animals show a huge diversity of adult body forms. To understand how unique morphologies were evolved is one of the most interesting issues of evolutionary biology. It is thought that these variations were acquired gradually by descent with modification (Darwin, 1859). Evolutionary developmental (EvoDevo) studies have been uncovering the genetic bases for variations of homologous tissues (Carroll et al., 2001). On the other hand, there are evolutionarily new characters which are never seen in other lineages. Such new characters are called novelty which is defined as “a new constructional element in a bodyplan that neither has a homologous counterpart in the ancestral species nor in the same organism” (Muller and Wagner, 1991). Many of novelties characterize specific taxa because these structures are conserved among descendants. That is, acquisition of novelty is the seeds of variation of the organism. However, the origin and evolutionary causes for novelty is still unknown in many structures. In this thesis, I investigated how animal development was modified for acquisition of novelty by focusing on the development of molluscs.

Mollusca is one of the most divergent animal phyla adapting to various

environment from deep sea to land (Ponder and Lindberg, 2008). Most molluscs form calcified shells on the dorsal side. Based on the shell morphologies, molluscs are grouped into eight classes. Recent genome-wide phylogenetic studies indicated that these eight classes are categorized into two higher groups; Aculifera and Conchifera (Kocot et al., 2011; Smith et al., 2011). Well-known taxa are included in the latter group, including Monoplacophora, Cephalopoda, Gastropoda, Scaphopoda and Bivalvia, while Chaetodermomorpha, Neomeniomorpha and Polyplacophora are classified into the former group. Common ancestors of the Conchifera are generally believed to possess a single shell on the dorsal side (Waller, 1998). The hard shell is an effective structure to protect the soft body from predators. However, the shell does not cover the whole body, allowing uptake of food/oxygen and the excretion of waste. To better protect the body against predators, gastropods and bivalves take distinct strategies. Gastropods acquired the operculum, which is formed in the posterior part of foot. On the other hand, bivalves separated shell into two plates. I focused on these two novel structures and investigated evolution of them by the methods of developmental biology

Early embryogenesis of molluscs has been studied for more than 100 years (Conklin, 1897; Lillie, 1895; Meisenheimer, 1901). Traditional studies indicated that

their early development is through spiral cleavage pattern, which is also observed in other phyla (Nielsen, 2010). In this type of cleavage, the first two divisions make four blastomeres, called A, B, C and D, which usually correspond to the left, ventral, right, and dorsal side of larvae, respectively (Dictus and Damen, 1997; Hejnol et al., 2007; Lillie, 1895; Render, 1991). After the four-cell stage, each four macromeres bud off a small micromere at its animal side. Each blastomere is labeled according to the rule proposed by Conklin (1897). For example, the D blastomere is divided into 1D macromere and 1d micromere. Because the orientation of the spindle is inclined, micromeres are displaced to the left or right of its sister macromere. After the generation of the first quartet of micromeres, the macromeres continue unequal cleavage to generate small micromeres on the animal side (1D is divided into 2D and 2d, and 1d is split into $1d^1$ and $1d^2$.). Moreover, fates of each blastomere are also well studied (Dictus and Damen, 1997; Hejnol et al., 2007; Henry et al., 2004; Lillie, 1895; Lyons et al., 2012; Render, 1991; Render, 1997). According to these studies, shell forming cells are mainly originated from 2d blastomere (Dictus and Damen, 1997; Hejnol et al., 2007; Henry et al., 2004; Lillie, 1895).

Although the cleavage pattern and the fate of blastomeres were well studied,

there were few studies for morphogenesis of molluscs by molecular techniques. Some studies reported genes which are expressed around the shell in the trochophore larvae stage (Hinman et al., 2003; Iijima et al., 2008; Jacobs et al., 2000; Kin et al., 2009; Nederbragt et al., 2002; Samadi and Steiner, 2009; Wanninger and Haszprunar, 2001). However, none of these genes has been examined by gene specific knockdown experiments. So there are still little understandings about molecular mechanism for shell morphogenesis of molluscs.

In the first chapter, I discussed mechanism for evolution of the operculum in gastropod based on the methods of molecular developmental biology including RNAi. In the second chapter, I tried to uncover the regulatory mechanism for early cleavage pattern which is thought to be related to the evolution of bivalve shell morphology.

Chapter 1:

The co-option of the *dpp* signaling pathway in the evolution of the operculum

Introduction

The operculum is one of the novelties in gastropods. It is a proteinaceous and sometimes calcified structure that is secreted by specific gland cells on the posterior part of the foot (Voltzow, 1994). Gastropods can protect their soft body perfectly against predators by blocking their shell opening with the operculum. Although some species, such as a limpet and a sea slug, do not have an operculum in adult stage, they form it in larval stage (Collier, 1997). Additionally, just as the shell coils in many gastropod species, the operculum also shows a spiral growth pattern. Thus, because the operculum shows notable similarities to the shell, there was an old argument stressing that the operculum was homologous with the shell, and that shell and operculum were together indicative of an original bivalve condition (Fleischmann, 1932; Gray, 1850). Here, including a test of the above hypothesis, I examined the evolutionary link between the shell plate and the operculum. In support of the link, several genes are expressed in both the shell field and the operculum, such as *ubfm* and *ferritin* (Jackson et al., 2007).

In all molluscan groups, the shell develops on the dorsal ectoderm (Kniprath, 1981). In gastropods, the first sign of shell morphogenesis is observed as shell-field invagination, which occurs at the gastrula stage as an invagination of dorsal epidermal cells (Kniprath, 1981; Nederbragt et al., 2002). Accompanied by shell matrix secretion into the invaginated extracellular space, shell-field cells evaginate, and subsequently, shell plate covers a wide area of the larval body (Kniprath, 1981). After the evagination of the shell field, cells along the margin of shell field are responsible for further secretion of the shell plate matrix. Histological observation of shell formation is well studied. On the other hand, there are few studies about operculum formation (Kano, 2006; Voltzow, 1994). The operculum is secreted by specific glands located on the posterior part of foot (Voltzow, 1994). However, there is no information when operculum glands differentiate or whether the operculum glands are developed from a part of shell glands. Several genes have been identified to be involved in the development of shell-field cells. *Engrailed* is expressed in cells responsible for shell matrix secretion in chitons, scaphopods, and bivalves as well as in gastropods (Iijima et al., 2008; Jacobs et al., 2000; Kin et al., 2009; Nederbragt et al., 2002; Wanninger and Haszprunar, 2001). *Hox1* has also been shown to be expressed in the shell-field margin of gastropods

(Hinman et al., 2003; Samadi and Steiner, 2009). In gastropods, *dpp* is expressed in cells surrounding the *engrailed*-positive cells (Iijima et al., 2008; Nederbragt et al., 2002). However, none of these genes has been examined in terms of function, such as through RNAi knockdown experiments.

To analyze the evolutionary link between the operculum and shell, I compared developmental process of them. First, I described development of the operculum glands histologically. Next, I compared gene expressions between shell glands and operculum glands. In addition to *engrailed*, *Hox1*, and *dpp*, I analyzed *grainyhead*. *grainyhead* is a transcription factor and has been proposed to have a conserved role in the differentiation of exocrine cells (Yamaguchi et al., 2006). Because the shell glands and operculum glands are both secretory organs, I reasoned that *grainyhead* may be involved in the development of both. As markers for shell and operculum glands, I used *ferritin* and *chitin synthase*. Ferritin is involved with shell calcification in chiton and bivalve (Kyung-Suk et al., 1986; Zhang et al., 2003), and expressed in both of shell and operculum glands in abalone (Jackson et al., 2007). Because chitin is the main component of shell and operculum matrix, I used *chitin synthase* as a glands marker. Finally, I performed gene function analysis by RNAi and discussed evolution of the

operculum.

Materials and Methods

Animals and in vitro fertilization

Sexually mature individuals of *Nipponacmea fuscoviridis* were collected in Yoshidahama Harbor, Miyagi Prefecture, Japan, during the breeding season (April–June and September–November). They were cultured in artificial sea water (ASW) at room temperature. In vitro fertilization was performed following the methods described by Deguchi (2007). Eggs and sperm were collected by cutting adult's foot and squeezing the gonads. To induce meiotic maturation, collected eggs were treated by ASW containing 5 mM NH_4Cl and 10 mM Tris-HCl (pH9.0) for 10 min. Eggs were washed by ASW three times, and incubated in ASW for about 1h. After fertilization, embryos were cultured in filtered sea water (FSW) at 22°C. Embryos were fixed in a solution containing 4% paraformaldehyde, 0.1 M MOPS (pH 7.5), 2 mM EGTA, and 0.5 M NaCl, and stored in 80% ethanol at -20°C.

Histology

Specimens were observed under Nomarsky optics using Nikon E-800. Matrix of shell plate and operculum were observed as refringent matrix under Nomarsky optics.

Fixed embryos were embedded in 2% agar. They were dehydrated through a graded ethanol series, which were then replaced by a graded ethanol-n-butanol series. Then, the agar blocks were embedded in paraffin. Sections (3 μm thick) were stained with Mayer's hematoxylin and eosin.

Cloning of genes and in situ hybridization

Using the primers shown in Table 1, *Nf-dpp*, *Nf-engrailed*, *Nf-Hox1*, *Nf-grainyhead*, *Nf-chitin synthase 1* (*Nf-CS1*), and *Nf-ferritin* were amplified with PCR. The primers were designed with reference to genome sequences from another species of limpet, *Lottia gigantia* (Simakov et al., 2013). GenBank/EMBL/DDBJ accession numbers are described in Table 1. In situ hybridization was performed as described by Kin et al. (2009). Digoxigenin-labeled RNA probes were synthesized in vitro from the cDNA clones using the Digoxigenin RNA labeling kit (Roche, Mannheim, BRD). After rehydration, embryos were treated by 2 μg/ml Proteinase K at 37°C for 20 min and then fixed in 4% paraformaldehyde for 1 hour. After prehybridization, the embryos were hybridized with digoxigenin-labeled probes at 55°C. The composition of hybridization buffer is as follows; 50% formamide, 6 × SSC, 5 × Denhart's solution, 900 μg/ml yeast

RNA, and 0.1% Tween 20. Excess probes were removed by washing the embryos twice in 50% formamide, 4 × SSC, and 0.1% Tween 20, twice in 50% formamide, 2 × SSC, and 0.1% Tween 20, and twice in 50% formamide, 1 × SSC, and 0.1% Tween 20. The embryos were incubated with 0.5% blocking reagent in PBT for 1 hour at room temperature. After blocking, embryos were incubated with alkaline phosphate-conjugated antidigoxigenin antibodies, and positive immunoreactions were visualized using Nitro blue tetrazolium/5-Bromo-4-chloro-3-indolyl phosphate (NBT/BCIP) solution (Roche, Mannheim, BRD).

Immunohistochemistry

After rehydration, the embryos were incubated in PBT with 3% BSA for 1 h. The specimens were incubated with 1/200 rabbit anti-FMRF-amid antibody (ImmunoStar, Hudson, WI, USA) in PBT for 1h. After rinsing four times in PBT, the samples were incubated with secondary antibody with Alexa 488 (Molecular Probes, Eugene, OR, USA) diluted 1/200 in PBT for 1 h. The samples were washed four times in PBS and mounted on slides in 50% glycerol in PBS for observation.

RNAi

Template cDNAs of each gene for double-stranded RNA (947 bp for *Nf-dpp* and 667 bp for the control *hedgehog* gene from the Japanese purple mussel, *Septifer virgatus)* were amplified using the primers shown in Table 1. Double-stranded RNA (dsRNA) was generated following Clemens et al. (2000). dsRNA dissolved in water was injected into fertilized eggs following Sweet et al. (2004). Microinjection was performed using micromanipulators (Narishige, Setagaya, Tokyo, JAP) and an injection apparatus (Femtojet; Eppendorf, Barkhausenweg, Hamburg, BRD). After injection, embryos were cultured in FSW (22°C) until fixed at 12, 16, or 20 h post-fertilization (hpf).

Results

Development of the operculum

First, I observed the developmental time-course of the shell and the operculum in *N. fuscoviridis*. At 8 hpf, the shell field was observed as a small invagination on the dorsal side (Fig. 1A and B). The ventral part was flat, and I could not find any sign of foot development or the operculum at this stage. At 10 hpf in the trochophore larva, when the shell-field invagination became more prominent, development of the foot began to be observed as a small protrusion in the ventral part (Fig. 1C and D). At 14 hpf, the shell field evaginated and expanded (Fig. 1E and F). Due to the expansion of the shell field, the telotroch moved upward and the mantle cavity began to form. At this stage, in the posterior part of the foot, I recognized cells of a distinct shape, specifically, long and columnar, oriented along the apical–basal axis (Fig. 1F). Note that the shell-field cells at 10 hpf showed a similar morphology (Fig. 1D). At 18 hpf in veliger larvae, the shell matrix covered a wide part of the body, and the mantle cavity became prominent (Fig. 1G and H). In the posterior part of the foot, I could recognize secretion of the operculum matrix, which was underlain by tall columnar cells (Fig. 1G and H).

Gene expression patterns

Expression of *Nf-engrailed* was detected in the shell-field margin and anterior ectoderm cells at the trochophore stage (10 hpf; Fig. 2A). At 14 hpf, as operculum development proceeded, expression was newly detected in the foot (black arrowhead in Fig. 2B). The signal persisted until 18 hpf, with the expression clear inside the foot and not in the epidermal layer (Fig. 2C). Thus, this *Nf-engrailed* expression did not mark cells involved in the matrix secretion of the operculum. FMRF-positive nerve cells were detected in a similar part of the foot at 22 hpf (white arrowhead in Fig. 2D), when *Nf-engrailed* expression was no longer detected. This suggests that this later expression of *Nf-engrailed* may be involved in neurogenesis in the foot ganglion.

Nf-dpp expression was detected in cells surrounding the shell field at 10 hpf (Fig. 3A). Subsequently, from 14 hpf, I detected new expression of *Nf-dpp* in the ventral epidermis of the foot (arrowhead in Fig. 3B). Expression in the shell-field margin was no longer detected at this stage. Expression in the posterior foot was detected at 18 hpf, when operculum matrix secretion was also observed. The cells underlying the operculum were marked by *Nf-dpp* expression (Fig. 3C).

I detected expression of *Nf-grainyhead* in the shell field and operculum glands.

At 10 hpf, expression was detected in cells adjacent to the shell field and in the most anterior region of shell field (Fig. 3D). At 14 hpf, expression was detected in the posterior part of the foot, and stronger expression was detected in a more limited part of the foot epithelium as the foot region grew bigger (Fig. 3E). At 18 hpf, expression was observed in cells underlying the operculum, but the expression was more restricted compared with *Nf-dpp* (Fig. 3F; compare with Fig. 3C).

The 10 hpf trochophore larvae show a half circle of *Nf-Hox1*-positive cells in the shell field (Fig. 3G). At the veliger stage (14–18 hpf), *Nf-Hox1* expression remained at the edge of the mantle, corresponding to the position of the shell glands, but I did not detect *Nf-Hox1* expression in the foot region (Fig. 3H and I).

I also examined developmental expression of two shell plate effector genes, *Nf-ferritin* and *Nf-chitin synthase 1* (*Nf-CS1*). At 10 hpf, both *Nf-ferritin* and *Nf-CS1* were expressed in cells surrounding the shell (Fig. 3J and M). At 14–18 hpf, expression of both genes were detected in the shell field margin, while only *Nf-ferritin* expression was detected in the operculum glands (Fig. 3K, L, N and O).

Function of *dpp* in the shell and operculum

Because *Nf-dpp* is expressed in the operculum as well as in the shell field margin, I examined the function of *Nf-dpp* in these organs. I found that inhibition of *Nf-dpp* by RNAi resulted in the failure of shell field development, which was not observed with a control RNAi using bivalve hedgehog (Fig. 4A and B, Table 2). I confirmed that 0.5 mg/ml of dsRNA was sufficient to degrade endogenous *Nf-dpp* (Fig. 5A and B, Table 3), and I performed further analyzes injecting this concentration of dsRNA. At this concentration, after injecting any dsRNAs, approximately 80% of larvae survived and kept swimming up to 20 hpf (Table 2). Among the survivors, the development of 10–20% larvae was apparently arrested at the trochophore stage (comparable to 10 hpf in normal development) and they failed to form a mantle cavity, although they continued to swim. When injected with *Nf-dpp*-dsRNA, more than half of the larvae (62/94: 66%, arrested larvae excluded) showed abnormal and smaller shell plates, whereas no such effect was observed in control dsRNA-injected larvae (Fig. 4 and Table 2). However, in *Nf-dpp*-dsRNA-injected larvae, some matrix was still observed (Fig. 4B), and thus shell development was not completely abolished. *Nf-CS1* expression was impaired in more than half of the injected larvae examined (14/23: Fig.

5G and H). Thus, *Nf-CS1* expression is likely to be under the control of *dpp* signaling. Expression of *Nf-grainyhead* in the shell-field margin was also severely affected in *Nf-dpp*-dsRNA-injected larvae; in most of the injected larvae (35/42), expression was not detected (Fig. 5M and N). On the other hand, expression of the other shell effector gene, *Nf-ferritin*, was unaffected (0/37: Fig. 5I and J). No effect was observed in the expression of *Nf-engrailed* or *Nf-Hox1* (Fig. 5C–F and Table 3). Thus, *Nf-dpp* appears to function in matrix secretion, where *Nf-CS1* is involved. However, secretion of some other matrix component in which ferritin is involved is not dependent on *dpp* signaling.

Operculum development was also impaired by *Nf-dpp*-dsRNA. In larvae surviving up to 20 hpf after being injected with 0.5 mg/ml *Nf-dpp*-dsRNA, approximately 40% of the larvae (47/117) showed no matrix secretion in the operculum, whereas the shell plate developed to some degree (Fig. 4B and D). No control dsRNA injected larvae showed such a phenotype without an operculum (Fig. 4A and C). Additionally, *Nf-grainyhead* expression was almost abolished in *Nf-dpp*-dsRNA larvae when examined at 16 hpf (24/29; Fig. 5O and P). However, expression of *Nf-ferritin* in the operculum was not affected (Fig. 5K and L), while morphology of the larvae was deformed due to the effect on shell field expansion. In addition, I observed tall columnar

cells in the posterior part of the foot even when dpp function of inhibited (Fig. 4D). Thus, *Nf-dpp* has certain roles for the matrix secretion in the operculum, but cell differentiation was not completely abolished by *Nf-dpp*-dsRNA.

Discussion

Developmental role of *dpp* in shell-field cell development

In this chapter, I provide evidence that *dpp* plays an important role in shell-field development. I found that expansion of mantle epithelium was significantly suppressed by *Nf-dpp*-dsRNA (Fig. 4). Cell proliferation of the shell-field margin is important for normal morphogenesis of gastropods to cover and protect the posterior body mass (Kniprath, 1981). In fact, Kurita (2011) showed *dpp* contributed cell proliferation in shell field in gastropod and bivalve. I also found that, although shell matrix secretion was not completely abolished by *Nf-dpp*-dsRNA, expression of one of the shell matrix effectors, *Nf-CS1*, was impaired (Fig. 5G and H). Thus, *Nf-dpp* signaling performs an important, but limited, role in shell matrix secretion. That is, shell matrix secretion is likely controlled in a complex and hierarchal manner. It is likely that *dpp* signaling is involved in certain aspect of matrix secretion, such as chitin synthesis. Shimizu et al. (2011) indicated that chemical inhibition of *dpp* signaling resulted in failure of calcification of the shell plate in pond snail. On the other hand, other aspects of shell development processes are not dependent on *dpp* signaling, such as the expression of *Nf-ferritin* (Fig. 5I and J). Several transcription factors are also

shown to be expressed in the shell field, including *Nf-engrailed* and *Nf-Hox1*. Although I tested inhibition of *Nf-dpp* expression by in situ hybridization (Fig. 5 and Table 3), *Nf-dpp* might be still expressed very low level which could not be detected by this method. Namely, abnormal shell formation might be due to low level expression of *Nf-dpp*. It is necessary to confirm by quantitative method such as qPCR whether *Nf-dpp* was completely abolished by RNAi. However, in *Nf-dpp*-dsRNA larvae, expression of *Nf-grainyhead* was not detected in 83% larvae, whereas expression of other transcription factors were expressed (Table 3). This result implied that there is another gene network for shell formation which is independent of *dpp* signaling. Indeed, *engrailed* shows conserved expression in the shell field of several molluscs (Jacobs et al., 2000; Kin et al., 2009; Nederbragt et al., 2002; Wanninger and Haszprunar, 2001); thus, it may perform a key role in shell formation. To understand shell development, future works on the function analysis of these genes should be necessary.

Development and evolution of the operculum

Because the operculum shows notable similarities with the shell, I explored the idea that co-option of the shell-field developmental process may account for the

evolution of the operculum by comparing developmental mechanisms of these two tissues. Development of the operculum begins at about 14 hpf with differentiation of thick cells in the posterior part of the foot (Fig. 1). In addition to the similarity in morphology of the thick columnar cells, I observed co-expression of *Nf-dpp*, *Nf-grainyhead*, and *Nf-ferritin* in both the operculum glands and the shell-field margin (Fig. 3). Inhibition of *Nf-dpp* signaling impaired matrix secretion in the shell and the operculum (Fig. 4). Because *dpp* signaling is involved in multiple contexts in animal development (Alberts et al., 2007), shared involvement of *dpp* cannot be a strong evidence for an evolutionary link. However, because the expression of *Nf-grainyhead* is dependent on *Nf-dpp* signaling in both the shell field and the operculum glands (Fig. 5M–P), it is probably safe to propose an evolutionary link in the developmental processes between the shell and the operculum. Thus, I suggest that co-option of the developmental process of the shell occurred during the evolution of the operculum.

My results may also be consistent with the idea that operculum originated from one of the bivalve shell plates (Fleischmann, 1932; Gray, 1850). However, histological data showed the operculum glands did not originate from a part of shell glands (Fig. 1). Also, I could not detect the expression patterns such that

Nf-dpp positive cells migrate from the shell field to operculum glands (Fig. 3). Rather the expression of *Nf-dpp* and *Nf-grainyhead* in operculum cells commences notably later than that in the shell glands (Fig. 3). Furthermore, lack of gene expression of *Nf-engrailed* or *Nf-Hox1* in the operculum glands does not support the origin of the operculum from one of the bivalve shells. Thus, my data are more consistent with co-option of the developmental process of the shell to the operculum. The co-option of *dpp–grainyhead* pathway may have contributed to providing a novel function, namely as matrix secretory cells, to the cells in the posterior part of foot. However, perhaps the co-option of the *dpp–grainyhead* pathway was insufficient, because *Nf-ferritin* expression is not under the control of *Nf-dpp* signaling in either the shell field or the operculum glands (Fig. 5I-L). Although *Nf-dpp* expression might not be abolished completely by RNAi, *Nf-ferritin* expression in *Nf-dpp* knockdown larvae suggests multiple regulatory cascades affect operculum formation. Thus, additional evolutionary events may have been required for the evolution of the operculum. Alternatively, co-option of a regulatory molecule further upstream of *dpp* might have occurred. In either case, co-option of the genetic cascade of *dpp–grainyhead* has provided a unique cellular nature as matrix secretors, and was an essential step for operculum evolution.

Such a phenomenon of shuffling the cellular nature within a body may be one of the major driving forces for the evolution of novel structures as expressed by Gould (1977) when he stated; “permutation of the old within complex systems can do wonders.” The innovation of the molluscan operculum is a typical example of a novel structure due to permutation of the old (shell).

Chapter 2:

The regulatory mechanism of the unique cleavage pattern of bivalves

Introduction

The calcified shell is one of the most characteristic structure of Mollusca. Each class of Mollusca is distinguished by the morphology of shell(s). During molluscan development, morphogenesis of the shell plate(s) initiates as early as the gastrula stage. In this stage, these are morphological differences between classes. Therefore, varieties in shell morphology in molluscs were likely achieved through modification during early embryogenesis.

Early embryogenesis of molluscs was first described more than 100 years ago (Conklin, 1897; Lillie, 1895; Meisenheimer, 1901). These studies indicated that molluscs develop through spiral cleavage patterns, which is also observed in other animal groups such as annelids. During spiral cleavage, the first two cleavages generate four blastomeres designated as A, B, C and D, which usually correspond to the left, ventral, right, and dorsal side of the larvae stage, respectively (Dictus and Damen, 1997; Hejnol et al., 2007; Lillie, 1895; Render, 1991). After the 4-cell stage, each macromere buds off a

small micromere at its animal side. Each quartet of micromeres is displaced to the right or left of its sister macromere. After generating the first quartet, the macromeres continue to divide unequally to generate animal micromere quartets. Thus, the largest cell in a cleavage stage is usually one of the macromeres located on the most vegetal side. This type of orthodox spiral cleavage is observed in gastropods, although some species possess larger D lineage blastomeres than other lineages due to asymmetric cell divisions, sometimes accompanied by the formation of the polar lobe. In either case, embryos develop into trochophore larvae with shell plates on the dorsal side.

Among Conchifera, bivalves acquired a novel body plan from their univalved ancestors via bilaterally separating the dorsal shell plate into two plates (Waller, 1998). The earliest sign of modification, which lead to the unique shell morphology of bivalves, is observed as early as the spiral cleavage stage.

In bivalves, most species show unequal cleavage during their first two cleavages and give rise to a larger D cell. This unequal cleavage is not unique to bivalves but is also observed in some species of gastropods or annelids (Nielsen, 2004). The first modification unique to bivalves is a reversal in polarity in the cleavage of the second D lineage micromere (cleavage of 2d and 2D). During orthodox spiral cleavage,

because the vegetal blastomere is usually larger, 2D is expected to be larger than 2d. However, for bivalves, 2d is larger than 2D, and the 2d blastomere derives a bivalve shell anlage (Lillie, 1895). According to the importance of the 2d cell and its descendants in bivalve development, the 2d cell and its largest descendant are denoted as X blastomere until bilateral division (Lillie, 1895). The 2d blastomere subsequently undergoes four unequal cleavages (Guerrier, 1970; Kin et al., 2009; Kurita et al., 2009; Lillie, 1895; Luetjens and Dorresteijn, 1995; Meisenheimer, 1901). The micromeres generated from X blastomeres are labeled X^1, X^2, X^3 and X^4 in order of their generation (Fig. 6A). The first two rounds of spiral cleavage are also unique and give rise to two small blastomeres on the vegetal side (X^1:$2d^2$ and X^2:$2d^{12}$). In the subsequent cleavage events, the polarity of X ($2d^{11}$) is reversed and gives rise to a small blastomere on the animal side (X^3: $2d^{111}$) and a large blastomere (X: $2d^{112}$) on the vegetal side. During the next cleavage, the cell size polarity is reversed again for the X blastomere ($2d^{112}$) and yields a small blastomere on the vegetal side (X^4: $2d^{1122}$). After these four unequal cleavages, the largest descendant of 2d (X; $2d^{1121}$) shows bilaterally symmetric cleavage. Interestingly, the bilateral daughter cells of X, $2d^{1121}$, were described as anlages of bilateral shell glands in bivalves (Lillie, 1895). Recently, it was suggested that some

descendants of the 1d blastomere and X^1 differentiate into ligament cells (Kin et al., 2009). Therefore, the unique cleavage pattern of the bivalves is associated closely with evolution of the bivalve body plan. Here, I explored how the unique cleavage is regulated and whether the cleavage pattern is regulated by an autonomous mechanism in D blastomere or is dependent on the interaction with other blastomeres. To accomplish this, I performed cell isolation experiments.

The development of isolated blastomeres has been studied extensively in gastropods since the first study was performed more than 100 years ago (Crampton and Wilson, 1896). Previous studies indicated that three or four rounds of spiral cleavage occur autonomously (Crampton and Wilson, 1896; Hess, 1956), and when isolated at the four-cell stage, D blastomere can develop shell glands (Cather, 1967). In addition, Cather (1967) provided evidence that shell glands differentiate from any animal blastomeres of the ectoderm through induction from vegetal blastomeres (Cather, 1967). However, in the bivalve *Mytilus*, Rattenbury and Berg (1954) reported that isolated D blastomere (or any other isolated blastomere) did not differentiate into shell glands (Rattenbury and Berg, 1954). Here, I re-examined this observation in another species of mussel, *Septifer virgatus*, using molecular markers for shell gland differentiation.

Materials and Methods

Animals and in vitro fertilization

Sexually mature individuals of *Septifer virgatus* were collected on the Hiraiso coast, Ibaraki Prefecture, Japan, during the breeding season (July-September). In vitro fertilization was performed following the methods described by Kurita et al. (2009). Embryos were cultured in ASW at 25˚C.

Cell isolation

To dissolve an egg membrane, sperm extracts were prepared as described previously (Berg, 1950). The two- or four-cell stage embryos were treated with sperm extract for 30 sec. After washing twice in ASW, embryos were separated by hand using a glass needle. Isolated blastomeres were collected in petri dishes. The cleavage pattern of isolated blastomeres was observed using a glass bottom dish (Matsunami Glass, Kishiwada, Oosaka, JPN). Embryos were cultured in ASW until fixation at 24 hpf.

Immunohistochemistry

The larvae were fixed with 4% paraformaldehyde, 0.1 M MOPS (pH 7.5), 2 mM

EGTA, and 0.5 M NaCl, and stored in 100% methanol at −20°C. After rehydration, the embryos were incubated in PBT with 3% BSA for 1 h. The specimens were incubated with 1/200 mouse anti-ß-tubulin antibody (Sigma, St. Louis, MO, USA) in PBT for 1h. After rinsing four times in PBT, the samples were incubated with secondary antibody with Alexa 555 (Molecular Probes, Eugene, OR, USA) diluted 1/200 in PBT for 1 h. The samples were washed four times in PBT and mounted on slides in 50% glycerol in PBS for observation.

In situ hybridization

In situ hybridization was performed as described the chapter 1. *Sv-Chitin synthase 1* (*Sv-CS1*) was cloned by PCR. GenBank/EMBL/DDBJ accession number and primers for PCR were shown in Table 1.

Results

Development of isolated AB and CD blastomeres

I first performed blastomere isolation at the 2-cell stage. For cell isolation, the egg membrane was dissolved using sperm extract treatment to reduce cell adhesion (Fig. 6B and C). The total numbers of isolated blastomeres were 503 for AB cells and 550 for CD cells. I observed cleavage pattern of a part of them under living conditions. A total of 87% (61/70 = cell cleavage events / cells observed) of the isolated AB cells divided into daughter cells of nearly the same size, while 90% (87/97) of CD cells divided unequally after forming the polar lobe (Fig. 7 and Movie.1). The remainder of the isolated blastomeres did not cleave, and no blastomeres showed abnormal cleavage patterns. These cleavage patterns of isolated blastomeres were similar to that of gastropods (Crampton and Wilson, 1896; Hess, 1956).

To examine further development, I fixed surviving larvae swimming by cilia at 24 hpf. The survival rate of embryos that developed from each blastomere of the 2-cell stage was 72% (361/503 = number of surviving larvae / number of isolated blastomeres) for AB and 73% (404/550) for CD. At this stage of normal development, larvae formed D-shape morphologies with separated shell plates covering a wide part of the body (Fig.

8A and B). Foot development was observed on the ventral side. The isolated AB blastomeres developed into trochophore-like larvae with prototroch, although I did not observe other structures such as the mouth, shell field, foot or apical tuft (Fig. 8C and D, and Table 4). Larvae from CD blastomere also developed into trochophore-like larvae with prototroch. The majority of larvae had shell plates on the dorsal side (Fig. 8E and F, and Table 4), but no foot-like structure was observed.

Cleavage pattern of isolated D blastomeres

To isolate D blastomeres, I treated 4-cell stage embryos with sperm extracts and isolated the largest blastomere (Fig. 6D and E). I could isolate 517 D blastomeres, and 174 cells of them were observed under living condition. Table 5 summarized the cleavage pattern of isolated D blastomeres. Among 174 isolated D blastomeres, 138 underwent two rounds of unequal cleavage (Fig. 9A). I considered the largest blastomere to be 2d (X). Although in some partial embryos, 2D and 1d were located on the same side as the large blastomere 2d, this was not indicative of a reversal of unequal cleavage (in spiral cleavage, blastomeres were located in the order 1d-2d-2D from the animal pole). Because the cleavage plane is oblique and the direction of

obliqueness reversed during successive cleavage, 1d and 2D are quite close during normal development (see Fig. 2B and H of Kurita et al. 2009 as well as Fig. 3 of Kin et al. 2009). A total of 14 embryos ended cleavage after one round of unequal cleavage, and 22/174 never underwent cleavage.

I further monitored the development of 138 embryos by focusing only on the subsequent cleavage pattern of X (2d) (Fig. 9, Movie 2 and Table 5). Among 138 embryos, 22 did not show any further cell division, and 26 stopped after one round of unequal cleavage. A total of 90 embryos showed two further rounds of unequal cleavage and two small blastomeres located adjacent to 2D (Fig. 9B and C). This cell arrangement is similar to that in normal development, in which X^1 ($2d^2$) and X^2 ($2d^{12}$) are located on the vegetal side of X ($2d^{11}$). A large number of isolated blastomeres ended cleavage at this stage, and only 40 embryos proceeded to the next round of unequal cleavage. During the next cleavage, the smaller blastomere emerged at the other side of the previous small blastomeres, perhaps reflecting the reversal of polarity during normal development, in which X ($2d^{11}$) divided unequally into small X^3 ($2d^{111}$) and larger X ($2d^{112}$) (Fig. 9E). A total of 17 blastomeres proceeded to the next round of unequal cleavage and gave rise to smaller blastomeres on the opposite side of the previous small blastomere. This also

likely reflects the cleavage of normal development, where X ($2d^{112}$) divided unequally into larger X ($2d^{1121}$) and smaller X^4 ($2d^{1122}$). After the above four rounds of unequal cleavages, 14 partial embryos showed a symmetric cell division, perhaps reflecting bilateral cleavage of X ($2d^{1121}$) into X^R ($2d^{11212}$) and X^L ($2d^{11211}$) (Fig. 9F). It should be noted that when focusing on the cleavage of X lineage, I did not observe blastomeres that underwent abnormal cleavage patterns.

Further development of isolated D-blastomeres and expression of *Sv-CS1*

The majority of isolated blastomeres stopped cell division of the X lineage midstream (only 14/138 proceeded to symmetric cell division of X ($2d^{1121}$)), but cell division did proceed in other cell lineages. Therefore, a significant number of isolated D-blastomeres could develop into swimming larvae. Indeed, 47% (241/517) of isolated D blastomeres survived and were swimming via cilia at 24 hpf. The morphology of larvae derived from D blastomeres was similar to that from CD (Fig. 8E-H). I observed an apical tuft, ciliary loop prototroch and shell plates (Table 4). While the ligament was clearly observed in un-operated larvae at this stage, I could not identify the ligament in larvae from isolated D blastomeres.

To further investigate shell development in larvae derived from D blastomeres, I examined the expression of *Sv-chitin synthase 1* (*Sv-CS1*). In the pacific oyster, chitin synthase is expressed in the mantle during the adult stage, and its expression started in the trochophore larvae stage (Zhang et al., 2012). Also, I showed *Nf-chitin synthase 1* is a good marker for the limpet's mantle edge in chapter 1 (Fig. 3M-O). During normal development of *S. virgatus*, the first weak signal of *Sv-CS1* was detected in the invaginated cells of the shell anlage at the early trochophore stage (Fig. 10A-C). After the shell field evaginated (14 hpf), *Sv-CS1* expression was detected at the mantle edge, and a new strong signal was observed in the ligament (Fig. 10D-F). At 16 hpf, *Sv-CS1* expression continued in the ligament as well as at the mantle edge (Fig. 10G-I). In 24 hpf larvae, strong *Sv-CS1* expression was observed at the mantle edge, while expression decreased in the ligament (Fig. 10J-L).

In the larvae derived from AB blastomeres, morphology was similar to that of early trochophores with prototroch, but I did not observe any sign of shell field invagination or mouth opening as described before (Fig. 8C). No samples of them showed *Sv-CS1* expression (0/32 = *Sv-CS1*-expressing larvae / analyzed larvae; Fig. 11A and B). On the other hand, in the larvae from D blastomeres, approximately half

(53/114) had *Sv-CS1*-positive cells on the dorsal side at 24 hpf (Fig. 11C-H). The majority of partial larvae derived from D blastomere failed to evaginate shell field cells. A total of 29/114 samples showed *Sv-CS1* expression in the invaginated cells (Fig. 11C and D), but 19/114 showed *Sv-CS1* signal outside of the invagination (Fig. 11E and F). Only five partial larvae showed evaginated shell plates, and the *Sv-CS1* signal was observed underlying the shell matrix (Fig. 11G and H). These observations indicated that shell field differentiation did not require an interaction with derivatives of A, B or C blastomeres.

Discussion

Shell field differentiation in isolated D blastomeres

In gastropods, blastomere isolation was performed extensively in the early 20th century to investigate mosaicism during early embryogenesis (Cather, 1967; Clement, 1962; Crampton and Wilson, 1896; Verdonk and Cather, 1973; Wilson, 1904). In these experiments, isolated D blastomeres could always form differentiated external shell. Some authors described that even other blastomeres (A, B or C), when isolated, developed an internal shell matrix (Cather et al., 1976; Verdonk and Cather, 1973). However, the "internal shell matrix" was later shown that the matrix was not necessarily indicative of differentiation of the shell matrix, but it may reflect abnormal specification of statocysts (McCain, 1992). I found that isolated D blastomeres can differentiate shell glands in bivalve (Fig. 11). However, this fact does not necessarily indicate that the shell gland can differentiate autonomously without any cell-cell interaction. Indeed, Cather (1967) indicated that, while isolated D blastomeres reached the veliger larvae stage with shell plates in *Ilyanassa*, depletion of vegetal blastomeres such as 2D or 3D resulted in loss of the shell plate. He also performed further experiments and demonstrated an inductive role of vegetal blastomeres for the

differentiation of shell glands. Blastomeres on the animal side when isolated at the 32-cell stage develop into hollow ball-like structure and do not differentiate into a shell gland. However, these animal blastomeres develop external shell matrices when combined with either macromere (3Q), mesentoblast, or even with isolated polar lobe. This induction of shell glands may account for the discrepancy in cell lineages between species. In most species, the shell glands originate from 2d blastomere, and the shell glands are derived from different lineages in some species, such as *Patella vulgata* (Dictus and Damen, 1997). Despite extensive studies in gastropods, blastomere isolation has rarely been performed in bivalves, and in a study using the mussel species *Mytilus edulis*, isolated D blastomeres did not develop shell plates (Rattenbury and Berg, 1954). In the present study, using another species of mussel, *Septifer virgatus*, I found that larvae from isolated D blastomeres express the shell gland marker *Sv-CS1* (Fig. 11) and secrete shell matrices (Fig. 8 and Table 4). This difference in isolated D blastomeres from different mussel species to develop shell plates may reflect different regulatory mechanisms between the two species, or it may be due to damage during experiments in the previous report. Future research will determine whether induction from vegetal blastomeres is also required for shell gland differentiation in bivalves.

Unique cleavage pattern of X blastomere is controlled autonomously

Bilateral separation of shell plates is a characteristic feature of bivalves. Previous studies indicated that the unique regulation of symmetric cell division following asymmetric cleavages of 2d lineage cells is closely associated with the unique morphology of shell plates (Kin et al., 2009; Lillie, 1895). In this study, I explored whether the unique cleavage pattern of 2d lineage is regulated autonomously or through interactions with other cells. I found that, even though a number of isolated D blastomeres end cleavage before bilateral cleavage, approximately 8% of isolated blastomeres followed the normal cleavage pattern up until bilateral cell division (Table 5). Notably I could not find any isolated blastomeres showing abnormal cleavage patterns, i.e., isolated blastomeres either ended cleavage or followed the normal cleavage pattern. Based on these observations, I concluded that the unique cleavage pattern did not require an interaction with cells originating from A, B or C blastomeres. Rather, the unique cleavage pattern is controlled by intrinsic mechanisms within the D lineage.

The regulatory mechanisms for asymmetric cell division are well-studied in model organisms, such as *Drosophila*, yeast and *C. elegans*, as well as in vertebrate cells

(Betschinger and Knoblich, 2004). These studies revealed a conserved regulatory mechanism for asymmetric cell division, where aPKC and Par proteins are localized in the specific site of the cell membrane and regulate asymmetric cell division by attracting centrosomes (Gonczy, 2008). These molecules are also thought to be involved in the regulation of asymmetric cleavage of early development in marine invertebrates such as ascidians and sea urchins (Alford et al., 2009; Patalano et al., 2006). Although involvement of these factors in the regulation of the unique cleavage of bivalves will be explored in future studies, the regulation of asymmetric cell division in bivalves may be more complicated than in sea urchin or ascidians. For ascidians and sea urchins, polarity of asymmetric cell division does not change during development; centrosomes are always pulled toward the vegetal pole in sea urchins (Dan, 1979) and towards the posterior pole in ascidians (Hibino et al., 1998). However, for 2d blastomere of bivalves, after giving rise to two micromeres on the vegetal side (X^1-$2d^2$ and X^2-$2d^{12}$), reversal of asymmetry occurs and produces micromeres on the animal side (X^3-$2d^{111}$). Subsequently, the reversal occurs again and produces a micromere on the vegetal side (X^4-$2d^{1122}$), prior to symmetric bilateral cleavage. I demonstrated that these reversals in asymmetry occur without interaction with other lineage cells (A, B or C lineages). Although it is

possible that the cell interaction with 2D lineage or 1d lineage cells regulate the reversal of asymmetry, my results suggested that D lineage blastomeres possess intrinsic mechanisms for counting cell division. Similar counting mechanisms were proposed for *Xenopus* mid-blastula transition (MBT) or ascidian muscle differentiation (Newport and Kirschner, 1982; Satoh and Ikegami, 1981). For the *Xenopus* MBT, the ratio between cytoplasmic vs. nuclear volumes is thought to be an important counting mechanism for initiating zygotic transcription in the mid-blastula stage (Newport and Kirschner, 1982). Ascidians were proposed to possess distinct counting mechanisms; they regulate the commitment to muscle differentiation based on the number of DNA replication cycles (Satoh and Ikegami, 1981). The reversal of asymmetric cell division in bivalve development can be used as a system to study the regulation of developmental timing. Furthermore, establishment of this unique mechanism may have been essential for evolution of the bivalve body plan.

General Discussion

In this thesis, I investigated the evolutionary mechanisms for acquisition of novelty in molluscs. The Mollusca is one of the most divergent phyla. Their developments show the spiral cleavage pattern and trochophore larvae, both phenomena are found in other phyla such as Annelida (Nielsen, 2004). Although morphologies of trochophore are similar between Mollusca and Annelida, remarkable differences are recognized in this stage among molluscan classes (Wanninger et al., 2008). Therefore, modification of cleavage pattern should strongly affect morphological differences of molluscs. This developmental pattern may not be general because variety of cleavage pattern is converged at phylotypic stages in vertebrates and arthropods (Slack et al., 1993). However, knowledge of molluscan morphogenesis should be essential piece for understanding diversification of animal form and its evolution.

In the first chapter, I investigated the evolutionary acquisition of the operculum in gastropod lineage. My results suggested that co-option of a part of the mechanisms for shell formation was important for acquisition of secretory ability of shell like matrices to operculum glands. However, *dpp* knockdown larvae had large cells on the posterior part of foot, their shape was similar to secretory cells (Fig. 4). Because

molluscs have many mucous glands on the epithelium, co-option of *dpp* signaling pathway might not add novel glands on the posterior part of foot but change the property of existing secretory cells. Interestingly, bivalves have unique glands on the posterior part of foot, called byssus glands (Brown, 1952). Bivalves anchor their body to rock by threadlike byssus, secreted from byssus glands (Yonge, 1962). The components of the operculum are more similar to that of byssus than shell components (Hunt, 1976). These similarities suspect that common ancestors of gastropods and bivalves had characteristic glands which were the origin of the operculum glands and the byssus glands. Even so, it is thought that co-option of *dpp* signaling pathway in the gastropod lineage is important for changing cell nature by integrating existing gene regulatory network.

The modification of cleavage pattern correlates with morphological difference of molluscs such as shell coiling in gastropod (Freeman and Lundelius, 1982) and two shell plates in bivalve (Lillie, 1895). As shown in chapter 2, unique cleavage pattern of D lineage in bivalves is regulated autonomously depending on the numbers of cleavage times. That is, it is assumed that bivalves regulate active state or movement of polarity factors depending on the numbers of cleavage times. Also, molluscs show dynamic

cytoplasmic movement, polar lobe formation. The factors in the polar lobe are important for differentiation of cell fate (Cather, 1967). It seems that molluscs can control the cytoplasmic movement strictly. Thus, molluscan blastomere can be used as a good model for study about the regulation of cytoplasmic movement.

Spiralian show conserved cleavage pattern and their determination of cell fate occurs in very early stage. Therefore it is possible to compare homologous blastomeres and their fate among the phylum, such as Mollusca and Annelida. These aspects are useful for EvoDevo researches such as how cell fate is developmentally determined and how cell type is evolutionally changed. I believe that researches about molluscan morphogenesis by cell biological and molecular developmental approaches will uncover evolutional and developmental mechanism for not only the diversified molluscan morphology but also the creation of variable shapes of organisms from simple egg.

Acknowledgements

I would like to express my cordial gratitude to Dr. Hiroshi Wada for his generous supports and critical discussions. I am deeply grateful to Dr. Kensuke Yahata and Dr. Masakazu Tokita for kind guidance of histological techniques. Dr. Ryusaku Deguchi kindly provided limpet samples. I received critical advice from Dr. Ryusuke Niwa about *grainyhead*. I would also like to express my appreciation to reviewers of this article, Dr. Masanao Honda, Dr. Yasunori Sasakura and Dr. Chikafumi Chiba. I would like to express special thanks to present and previous lab members especially Dr. Yoshihisa Kurita and Mrs. Kana Murakami. I also thank Aqua World Ibaraki Prefectural Oarai Aquarium for supplying sea water. Research grants from Japan Science Society (23-451) and Japan Society for the Promotion of Science (12J01644) funded this work.

References

Alberts, B., Johnson, A., Lewis, J., Raff, M., Roberts, K., Walter, P., 2007. Molecular Biology of the Cell. Garland Science, New York.

Alford, L. M., Ng, M. M., Burgess, D. R., 2009. Cell polarity emerges at first cleavage in sea urchin embryos. Developmental Biology. 330, 12-20.

Berg, W. A., 1950. Lytic effects of sperm extracts on the eggs of *Mytilus edulis*. The Biological Bulletin. 98, 128-138.

Betschinger, J., Knoblich, J. A., 2004. Dare to be different: asymmetric cell division in *Drosophila*, *C. elegans* and Vertebrates. Current Biology. 14, R674-R685.

Brown, C. H., 1952. Some structural proteins of *Mytilus edulis*. Quarterly Journal of Microscopical Science. s3, 487-502.

Carroll, S. B., Grenier, J. K., Weatherbee, S. D., 2001. From DNA to diversity: molecular genetics and the evolution of animal design. Blackwell Science, Massachusetts.

Cather, J. N., 1967. Cellular interactions in the development of the shell gland of the gastropod, *Ilyanassa*. Journal of Experimental Zoology. 166, 205-223.

Cather, J. N., Verdonk, N. H., Dohmen, M. R., 1976. Role of the vegetal body in the regulation of development in *Bithynia tentaculata* (Prosobranchia, Gastropoda).

American Zoologist. 16, 455-468.

Clemens, J. C., Worby, C. A., Simonson-Leff, N., Muda, M., Maehama, T., Hemmings, B. A., Dixon, J. E., 2000. Use of double-stranded RNA interference in *Drosophila* cell lines to dissect signal transduction pathways. Proceedings of the National Academy of Sciences of the United States of America. 97, 6499-6503.

Clement, A. C., 1962. Development of *Ilyanassa* following removal of the D macromere at successive cleavage stages. Journal of Experimental Zoology. 149, 193-215.

Collier, J. R., Gastropods, the snails. In: S. F. Gilbert, A. M. Raunio, Eds.), Embryology, constructing the organism. Sinauer Assoc., Sunderland, MA 1997, pp. 189-218.

Conklin, E. G., 1897. The embryology of *Crepidula*. Journal of Molphology. 13, 3-209.

Crampton, H. E., Wilson, E. B., 1896. Experimental studies on gasteropod development. Archiv für Entwicklungsmechanik der Organismen. 3, 1-19.

Dan, K., 1979. Studies on unequal cleavage in sea urchins I. Migration of the nuclei to the vegetal pole. development, Growth & Differentiation. 21, 527-535.

Darwin, C., 1859. On the origin of species by means of natural selection, or the preservation of favoured races in the struggle for life. John Murray.

Deguchi, R., 2007. Fertilization causes a single Ca^{2+} increase that fully depends on Ca^{2+}

influx in oocytes of limpets (Phylum Mollusca, Class Gastropoda). Developmental Biology. 304, 652-663.

Dictus, W. J. A. G., Damen, P., 1997. Cell-lineage and clonal-contribution map of the trochophore larva of *Patella vulgata* (Mollusca). Mechanisms of Development. 62, 213-226.

Fleischmann, A., 1932. Vergleichende betrachtungen über das schalenwachstum der weichtiere (mollusca). Zoomorphology. 25, 549-622.

Freeman, G., Lundelius, J., 1982. The developmental genetics of dextrality and sinistrality in the gastropodLymnaea peregra. Wilhelm Roux's archives of developmental biology. 191, 69-83.

Gonczy, P., 2008. Mechanisms of asymmetric cell division: flies and worms pave the way. Nature Reviews Molecular Cell Biology. 9, 355-366.

Gould, S. J., 1977. Ontogeny and phylogeny. The Belknap Press of Harvard University Press, Cambridge.

Gray, J. E., 1850. On the operculum of gastropodous Mollusca, and an attempt to prove that it is homologous or identical with the second valve of Conchifera. Annals and Magazine of Natural History. 5, 475-483.

Guerrier, P., 1970. Les caractères de la segmentation et la détermination de la polarité dorsoventrale dans le développement de quelques Spiralia III. *Pholas dactylus* et *Spisula subtruncata* (Mollusques Lamellibranches). Journal of Embryology and Experimental Morphology. 23, 667-692.

Hejnol, A., Martindale, M. Q., Henry, J. Q., 2007. High-resolution fate map of the snail *Crepidula fornicata*: The origins of ciliary bands, nervous system, and muscular elements. Developmental Biology. 305, 63-76.

Henry, J., Okusu, A., Martindale, M., 2004. The cell lineage of the polyplacophoran, *Chaetopleura apiculata*: variation in the spiralian program and implications for molluscan evolution. Developmental Biology. 272, 145-160.

Hess, O., 1956. Die entwicklung von halbkeimen bei dem süsswasser-prosobranchier *Bithynia tentaculata* L. Wilhelm Roux' Archiv für Entwicklungsmechanik der Organismen. 148, 336-361.

Hibino, T., Nishikata, T., Nishida, H., 1998. Centrosome-attracting body: a novel structure closely related to unequal cleavages in the ascidian embryo. Development, Growth & Differentiation. 40, 85-95.

Hinman, V. F., O'Brien, E. K., Richards, G. S., Degnan, B. M., 2003. Expression of anterior

Hox genes during larval development of the gastropod *Haliotis asinina*. Evolution & Development. 5, 508-521.

Hunt, S., 1976. The gastropod operculum: a comparative study of the composition of gastropod opercular proteins. Journal of Molluscan Studies. 42, 251-260.

Iijima, M., Takeuchi, T., Sarashina, I., Endo, K., 2008. Expression patterns of *engrailed* and *dpp* in the gastropod *Lymnaea stagnalis*. Development Genes and Evolution. 218, 237-251.

Jackson, D. J., Wörheide, G., Degnan, B. M., 2007. Dynamic expression of ancient and novel molluscan shell genes during ecological transitions. BMC Evolutionary Biology. 7, 160.

Jacobs, D. K., Wray, C. G., Wedeen, C. J., Kostriken, R., DeSalle, R., Staton, J. L., Gates, R. D., Lindberg, D. R., 2000. Molluscan *engrailed* expression, serial organization, and shell evolution. Evolution & Development. 2, 340–347.

Kano, Y., 2006. Usefulness of the opercular nucleus for inferring early development in neritimorph gastropods. Journal of Morphology. 267, 1120-1136.

Kin, K., Kakoi, S., Wada, H., 2009. A novel role for *dpp* in the shaping of bivalve shells revealed in a conserved molluscan developmental program. Developmental Biology.

329, 152-166.

Kniprath, E., 1981. Ontogeny of the molluscan shell field - a review. Zoologica Scripta. 10, 61-79.

Kocot, K. M., Cannon, J. T., Todt, C., Citarella, M. R., Kohn, A. B., Meyer, A., Santos, S. R., Schander, C., Moroz, L. L., Lieb, B., Halanych, K. M., 2011. Phylogenomics reveals deep molluscan relationships. Nature. 477, 452-456.

Kurita, Y., Evolution of the molluscan bodyplan brought by the alteration of early developmental process. Structural biosciences, Vol. doctor of philosophy in science. University of Tsukuba, Ibaraki, 2011.

Kurita, Y., Deguchi, R., Wada, H., 2009. Early development and cleavage pattern of the Japanese purple mussel, *Septifer virgatus*. Zoological Science. 26, 814-820.

Kyung-Suk, K., Webb, J., Macey, D. J., 1986. Properties and role of ferritin in the hemolymph of the chiton *Clavarizona hirtosa*. Biochimica et Biophysica Acta (BBA) - General Subjects. 884, 387-394.

Lillie, F. R., 1895. The embryology of the Unionidae. Journal of Morphology. 10, 1-100.

Luetjens, C. M., Dorresteijn, A. W. C., 1995. Multiple, alternative cleavage patterns precede uniform larval morphology during normal development of *Dreissena polymorpha*

(Mollusca, Lamellibranchia). Rouxs Archives of Developmental Biology. 205, 138-149.

Lyons, D. C., Perry, K. J., Lesoway, M. P., Henry, J. Q., 2012. Cleavage pattern and fate map of the mesentoblast, 4d, in the gastropod *Crepidula*: a hallmark of spiralian development. EvoDevo. 3, 21.

McCain, E. R., 1992. Cell interactions influence the pattern of biomineralization in the *Ilyanassa obsoleta* (Mollusca) embryo. Developmental Dynamics. 195, 188-200.

Meisenheimer, J., 1901. Entwicklungsgeschichte von Dreissensia polymorpha Pall. Zeitschrift für Wissenschaftliche Zoologie. 69, 1-137.

Muller, G. B., Wagner, G. P., 1991. Novelty in evolution: restructuring the concept. Annual Review of Ecology and Systematics. 22, 229-256.

Nederbragt, A., Loon, A. E. v., Dictus, W. J. A. G., 2002. Expression of *Patella vulgata* orthologs of *engrailed* and *dpp-BMP2/4* in adjacent domains during molluscan shell development suggests a conserved compartment boundary mechanism. Developmental Biology. 246, 341-355.

Newport, J., Kirschner, M., 1982. A major developmental transition in early *Xenopus* embryos I. Characterization and timing of cellular changes at the midblastula stage.

Cell. 30, 675-686.

Nielsen, C., 2004. Trochophora larvae: Cell-lineages, ciliary bands, and body regions. 1. Annelida and Mollusca. Journal of Experimental Zoology. 302B, 35-68.

Nielsen, C., 2010. Some aspects of spiralian development. Acta Zoologica. 91, 20-28.

Patalano, S., Prulière, G., Prodon, F., Paix, A., Dru, P., Sardet, C., Chenevert, J., 2006. The aPKC-PAR-6-PAR-3 cell polarity complex localizes to the centrosome attracting body, a macroscopic cortical structure responsible for asymmetric divisions in the early ascidian embryo. Journal of Cell Science. 119, 1592-1603.

Ponder, W. F., Lindberg, D. R., 2008. Phylogeny and Evolution of the Mollusca. Univ of California Press.

Rattenbury, J. C., Berg, W. E., 1954. Embryonic segregation during early development of *Mytilus edulis*. Journal of Morphology. 95, 393-414.

Render, J., 1991. Fate maps of the first quartet micromeres in the gastropod *Ilyanassa obsoleta*. Development. 113, 495-501.

Render, J., 1997. Cell fate maps in the *Ilyanassa obsoleta* embryo beyond the third division. Developmental Biology. 189, 301-310.

Samadi, L., Steiner, G., 2009. Involvement of Hox genes in shell morphogenesis in the

encapsulated development of a top shell gastropod (*Gibbula varia* L.). Development Genes and Evolution. 219, 523-530.

Satoh, N., Ikegami, S., 1981. A definite number of aphidicolin-sensitive cell-cyclic events are required for acetylcholinesterase development in the presumptive muscle cells of the ascidian embryos. Journal of Embryology and Experimental Morphology. 61, 1-13.

Shimizu, K., Sarashina, I., Kagi, H., Endo, K., 2011. Possible functions of Dpp in gastropod shell formation and shell coiling. Development Genes and Evolution. 221, 59-68.

Simakov, O., Marletaz, F., Cho, S.-J., Edsinger-Gonzales, E., Havlak, P., Hellsten, U., Kuo, D.-H., Larsson, T., Lv, J., Arendt, D., Savage, R., Osoegawa, K., de Jong, P., Grimwood, J., Chapman, J. A., Shapiro, H., Aerts, A., Otillar, R. P., Terry, A. Y., Boore, J. L., Grigoriev, I. V., Lindberg, D. R., Seaver, E. C., Weisblat, D. A., Putnam, N. H., Rokhsar, D. S., 2013. Insights into bilaterian evolution from three spiralian genomes. Nature. 493, 526-531.

Slack, J. M. W., Holland, P. W. H., Graham, C. F., 1993. The zootype and the phylotypic stage. Nature. 361, 490-492.

Smith, S. A., Wilson, N. G., Goetz, F. E., Feehery, C., Andrade, S. C. S., Rouse, G. W., Giribet, G., Dunn, C. W., 2011. Resolving the evolutionary relationships of molluscs with

phylogenomic tools. Nature. 480, 364-367.

Sweet, H., Amemiya, S., Ransick, A., Minokawa, T., McClay, D. R., Wikramanayake, A., Kuraishi, R., Kiyomoto, M., Nishida, H., Henry, J., Blastomere isolatio and transplantation. In: C. A. Ettensohn, G. M. Wessel, G. A. Wray, Eds.), Development of sea urchins, ascidianas, and other invertebrate deuterostomes: experimental approaches. Elsevier Academic Press, San Diego, 2004.

Verdonk, N. H., Cather, J. N., 1973. The development of isolated blastomeres in *Bithynia tentaculata* (Prosobranchia, Gastropoda). Journal of Experimental Zoology. 186, 47-61.

Voltzow, J., Gastropoda: Prosobranchia. In: F. W. Harrison, A. J. Kohn, Eds.), Microscopic Anatomy of Invertebrates, Mollusca Ⅰ. Wiley-Liss, Inc, 1994, pp. 111-252.

Waller, T. R., Origin of the molluscan class Bivalvia and a phylogeny of major groups. In: P. A. Johnston, J. W. Haggart, Eds.), Bivalves: an eon of evolution. . University of Calgary Press., Calgary, 1998, pp. 1-45.

Wanninger, A., Haszprunar, G., 2001. The expression of an engrailed protein dring embryonic shell formation of the tusk-shell, *Antalis entalis* (Mollusca, Scaphopoda). Evolution & Development. 3, 312-321.

Wanninger, A., Koop, D., Moschel-Lynch, S., Degnan, B. M., Molluscan evolutionary development. In: W. F. Ponder, D. R. Lindberg, Eds.), Phylogeny and evolution of the Mollusca. University of California Press, Berkeley, 2008, pp. pp. 427-445.

Wilson, E. B., 1904. Experimental studies in germinal localization II. Experiments on the cleavage-mosaic in *Patella* and *Dentalium*. Journal of Experimental Zoology. 1, 197-268.

Yamaguchi, Y., Yonemura, S., Takada, S., 2006. Grainyhead-related transcription factor is required for duct maturation in the salivary gland and the kidney of the mouse. Development. 133, 4737-4748.

Yonge, C. M., 1962. On the primitive significance of the byssus in the Bivalvia and its effects in evolution. Journal of the Marine Biological Association of the United Kingdom 42, 113-125.

Zhang, G., Fang, X., Guo, X., Li, L., Luo, R., Xu, F., Yang, P., Zhang, L., Wang, X., Qi, H., Xiong, Z., Que, H., Xie, Y., Holland, P. W., Paps, J., Zhu, Y., Wu, F., Chen, Y., Wang, J., Peng, C., Meng, J., Yang, L., Liu, J., Wen, B., Zhang, N., Huang, Z., Zhu, Q., Feng, Y., Mount, A., Hedgecock, D., Xu, Z., Liu, Y., Domazet-Loso, T., Du, Y., Sun, X., Zhang, S., Liu, B., Cheng, P., Jiang, X., Li, J., Fan, D., Wang, W., Fu, W., Wang, T., Wang, B.,

Zhang, J., Peng, Z., Li, Y., Li, N., Chen, M., He, Y., Tan, F., Song, X., Zheng, Q., Huang, R., Yang, H., Du, X., Chen, L., Yang, M., Gaffney, P. M., Wang, S., Luo, L., She, Z., Ming, Y., Huang, W., Huang, B., Zhang, Y., Qu, T., Ni, P., Miao, G., Wang, Q., Steinberg, C. E., Wang, H., Qian, L., Liu, X., Yin, Y., 2012. The oyster genome reveals stress adaptation and complexity of shell formation. Nature. 490, 49-54.

Zhang, Y., Meng, Q., Jiang, T., Wang, H., Xie, L., Zhang, R., 2003. A novel ferritin subunit involved in shell formation from the pearl oyster (*Pinctada fucata*). Comparative Biochemistry and Physiology Part B: Biochemistry and Molecular Biology.

Tables

Table 1

Accession numbers and primers used for PCR.

Gene names	Accession numbers	Primers (upper: forward, lower: revers)
Nf-dpp	AB612238	GCCAACACAGTTCGCAGCTTTTA ACCATATCTTGATAGTTTTTAAGCAC
Nf-engrailed	AB639757	AACTTTTCTATAGCAGAAATT TTGTGATTGTAAAGTCCTTCCGAC
Nf-Hox1	AB639756	GATTATACGCTTTGCAATTTG TTCACGCATGCGCTTCTTTTG
Nf-grainyhead	AB639758	CTAGAATCACCTATCTCAACTA TTTTATATTTCTCTTCAATAGC
Nf-ferritin	AB639755	CAACCACGTCAAAACTTCCAT GTATTCACCCAGACCAGTTCC
Nf-chitin synthase 1	AB646432	ACAGGAAATGACGCAACTTCTCA TTGAAATCAACATCACCATCCAA
Sv-chitin synthase 1	AB613818	ATGAAAAGTGACATTCAGATTGGCAG TCTGGTTCCCATCCAGGAGGAACAACATC
Nf-dpp-dsRNA	–	TAATACGACTCACTATAGGGCGAAACACAGTTCGCAGCTTTTACCATAACG TAATACGACTCACTATAGGGCGACCATATCTTGATAGTTTTTAAGCACAAC
Sv-hedgehog -dsRNA	–	TAATACGACTCACTATAGGGCGATGTATTACGAATCACG TAATACGACTCACTATAGGGCGACAGAGTTATTGTTAAT

Table 2

Effect of *Nf-dpp* RNAi on the larval morphology at 20 hpf of *N. fuscoviridis*.

	No. of injected	survived larvae	Normal	shell_ab, Op._+	shell_ab, Op._−	shell_ − , Op._−
Control dsRNA	96	84	73	0	0	11
Nf-dpp dsRNA	145	117	32	15	47	23

Shell_ab.: abnormal shape of shell, Shell_−: shell absent,

Op._+: operculum present, Op._−: operculum absent.

Table 3

Effect of *Nf-dpp* RNAi on gene expressions.

(Number of larvae in which expression was not detected/number of examined larvae)

	Nf-dpp	*Nf-en*	*Nf-Hox1*	*Nf-grh*	*Nf-CS1*	*Nf_fer*	*Nf_grh*	*Nf_fer*
	12 hpf (shell field)						16 hpf (operculum)	
Control dsRNA	2/25	0/35	0/32	0/42	0/63	0/22	0/41	0/21
Nf-dpp-dsRNA	43/46	0/58	0/69	35/42	14/23	0/37	24/29	0/18

Nf-en: *Nf-engrailed*, *Nf-grh*: *Nf-grainyhead*, *Nf-fer*: *Nf-ferritin*

Table 4

Effect of cell isolation on the larval morphology at 24 hpf of *S.virgatus*.

Isolated blastomere	No. of samples	ciliary loop	apical tuft	shell	mouth
AB	19	19	0	0	0
CD	20	20	15	13	12
D	26	26	15	17	16

Table 5

The successful number of X lineage cleavage.

Total number	1d-1D	X (2d)	X^1 ($2d^2$)	X^2 ($2d^{12}$)	X^3 ($2d^{111}$)	X^4 ($2d^{1122}$)	X^L&X^R
174	152	138	116	90	40	17	14
%	87.3	79.3	66.7	51.7	23	9.8	8

Figures and Legends

Fig. 1. Outline of development of the shell and operculum in *N. fuscoviridis*.

(A, B) At 8 hpf, the shell field was observed as a small invagination on the dorsal side. However, no sign of foot development was observed. Lateral view (A, dorsal to the left) and dorsal view (B). Shell field is encircled by white broken lines. (C, D) At 10 hpf, the shell-field invagination was more prominent, and foot development was observed as a small protrusion in the ventral part. Lateral view of whole-mount larvae (C) and sectioned image (D). Dorsal to the left. Shell field is encircled by white broken lines. (E, F) The shell plate matrix was first observed in 14 hpf early veliger larvae. Due to the expansion of the mantle epithelium, the foot moved upward, and a mantle fold emerged. Operculum cells were observed as long cells in the posterior part of the foot (encircled by black broken line). Lateral view of whole-mount larvae (E) and sectioned image (F). Dorsal to the left. (G, H) At 18 hpf, the shell plate developed with a dome-like shape and surrounded a wide part of the larval body. The matrix of the operculum also emerged at this stage (white arrowhead). Lateral view of whole-mount larvae (G) and sectioned image (H). Dorsal to the left. Black arrows: foot, white arrows: mantle edge, white arrowhead: operculum. Scale bars: 20 μm.

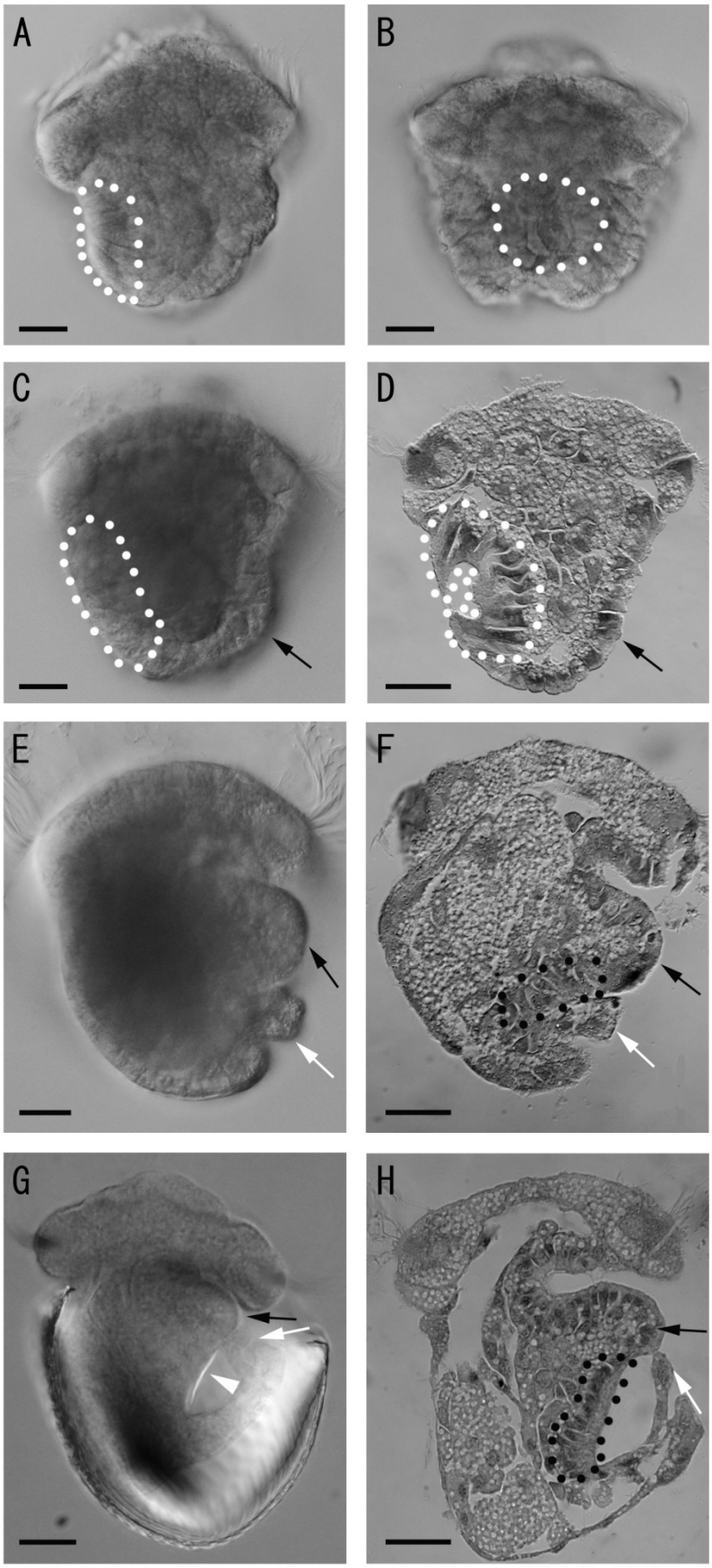
A
B
C
D
E
F
G
H

Fig. 2. Expression pattern of *Nf-engrailed* and FMRF-amide.

(A) *Nf-engrailed* was expressed in the edge of shell field and anterior ectoderm cells (arrows) at the 10 hpf trochophore larva (dorsal view). (B) At 14 hpf, new *Nf-engrailed* signals were observed in the foot indicated by black arrowhead (lateral view). (C) At 18 hpf, expression of *Nf-engrailed* was observed in the anterior cells (arrow) and inside of the foot (black arrowhead) not in mantle edge (lateral view). (D) FMRF-amid positive nerve cells were located in the foot pointed by white arrowhead at 22 hpf. Asterisks indicate non-specific staining of shell. Scale bars: 50 μm.

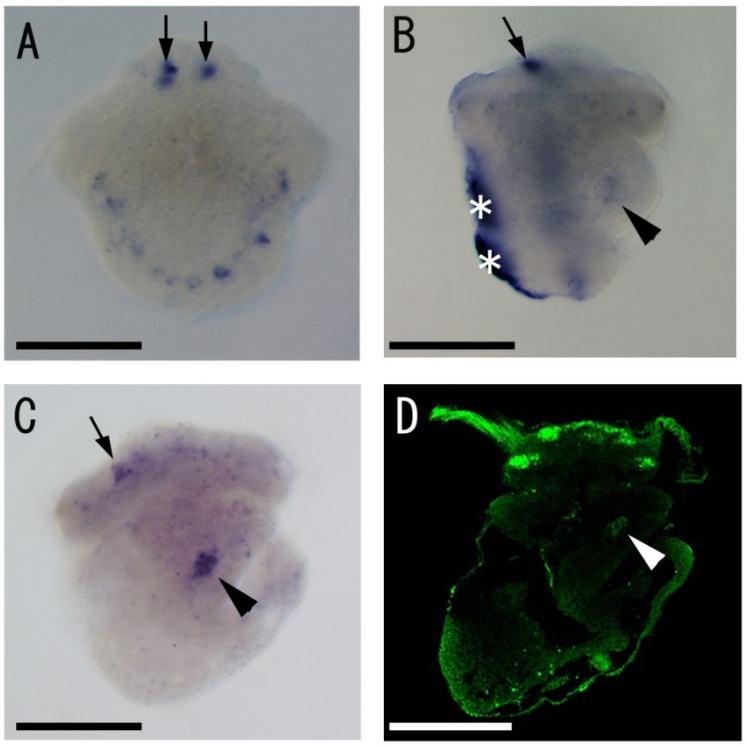
A
B
C
D

Fig. 3. Expression pattern of *Nf-dpp*, *Nf-grainyhead Nf-Hox1*, *Nf-ferritin* and *Nf-CS1.*

Expression patterns of *Nf-dpp* (A–C), *Nf-grainyhead* (D–F), *Nf-Hox1* (G–I), *Nf-ferritin* (J–L) and *Nf-CS1* (M–O). Dorsal view of the 10 hpf trochophore larvae (A, D, G, J, M). Lateral views at 14 hpf (B, E, H, K, N) and 18 hpf (C, F, I, L, O). Dorsal to the left. The expressions in the operculum glands are indicated by black arrowheads. Asterisks indicate non-specific staining of shell plate. Scale bars: 50μm.

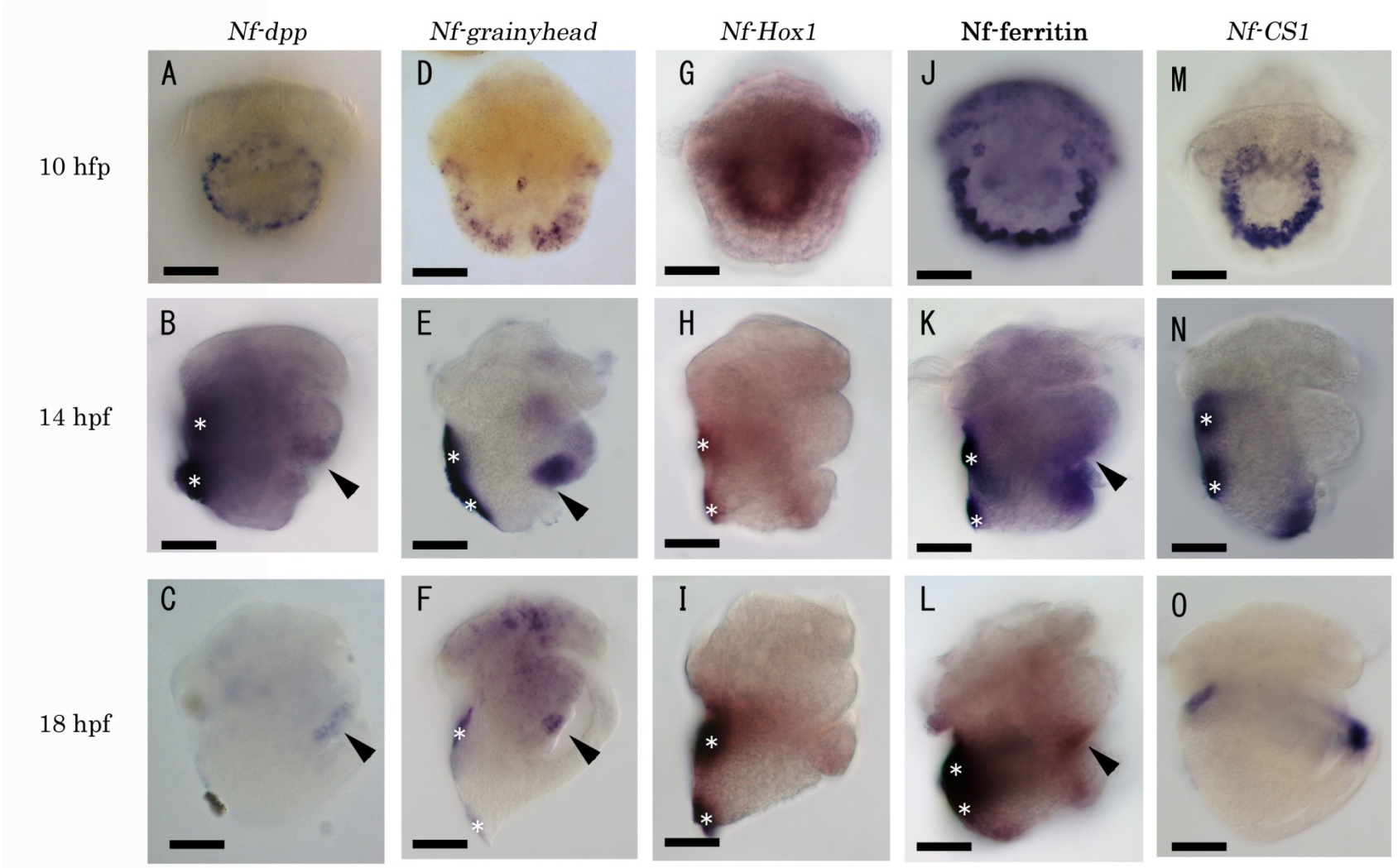
Nf-dpp
Nf-grainyhead
Nf-Hox1
Nf-ferritin
Nf-CS1
10 hfp
14 hpf
18 hpf
A
B
C
D
E
F
G
H
I
J
K
L
M
N
O

Fig. 4. Effect of *Nf-dpp* dsRNA on larval morphology.

(A) Morphology of control dsRNA-injected larva at 20 hpf. (B) Morphology of *Nf-dpp* dsRNA larva at 20 hpf. (C, D) Enlarged images of the foot region of the larvae are shown in (A) and (B), respectively. Operculum region is indicated by arrowheads. Clear operculum matrix was observed in control larvae (C), but no matrix was observed in *Nf-dpp* dsRNA larvae, while tall columnar cells were still observed as indicated by arrowheads (D). pt: prototroch, f: foot. Scale bars: 50 μm.

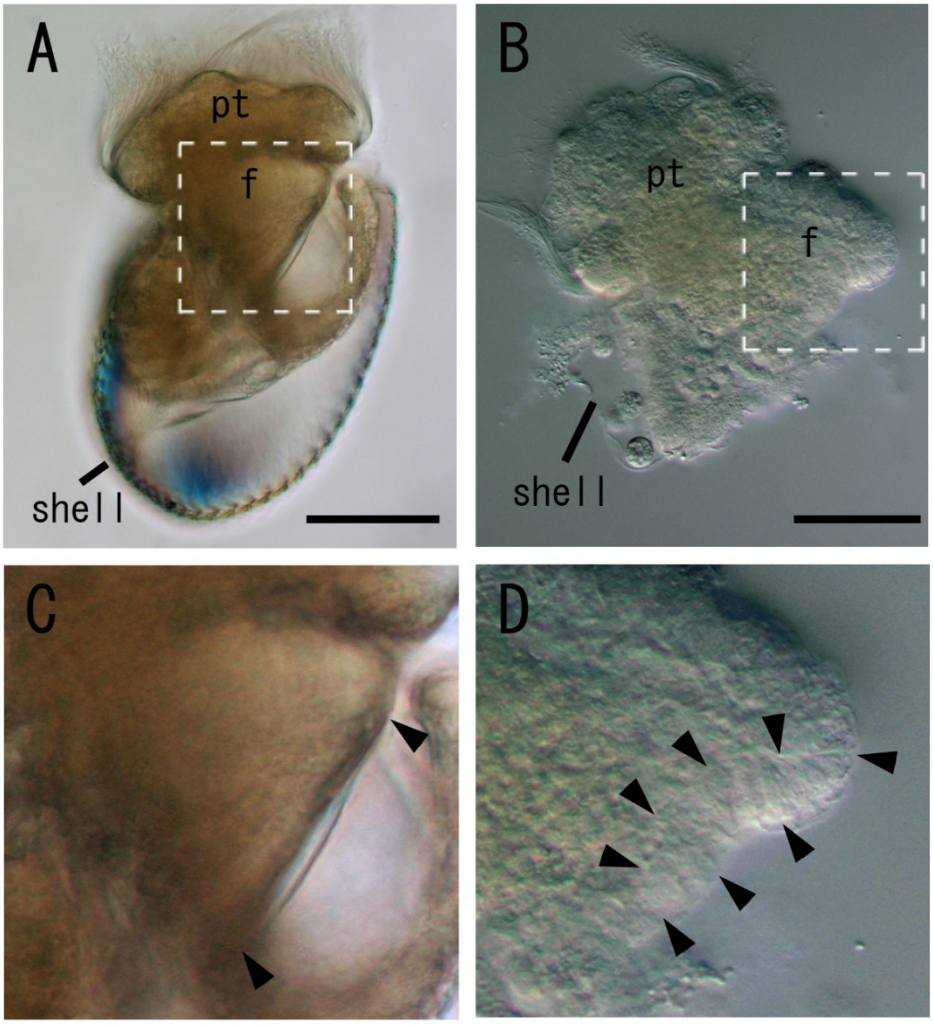
A
pt
f
shell
B
pt
f
shell
C
D

Fig. 5. Effect of *Nf-dpp*-dsRNA on gene expressions.

Expression of *Nf-dpp* (A, B), *Nf-engrailed* (C, D), *Nf-Hox1* (E, F), *Nf-CS1* (G, H), *Nf-ferritin* (I–L) and *Nf-grainyhead* (M–P) in control dsRNA-injected larvae (A, C, E, G, I, K, M, O) or *Nf-dpp*-dsRNA-injected larvae (B, D, F, H, J, L, N, P). Expression was examined at the 12 hpf trochophore stage (A–J, M, N: dorsal views) or the 16-hpf veliger stage (K, L, O, P: lateral views, dorsal to the left). Arrowheads indicate the position of the operculum cells. Asterisks indicate non-specific staining of shell.

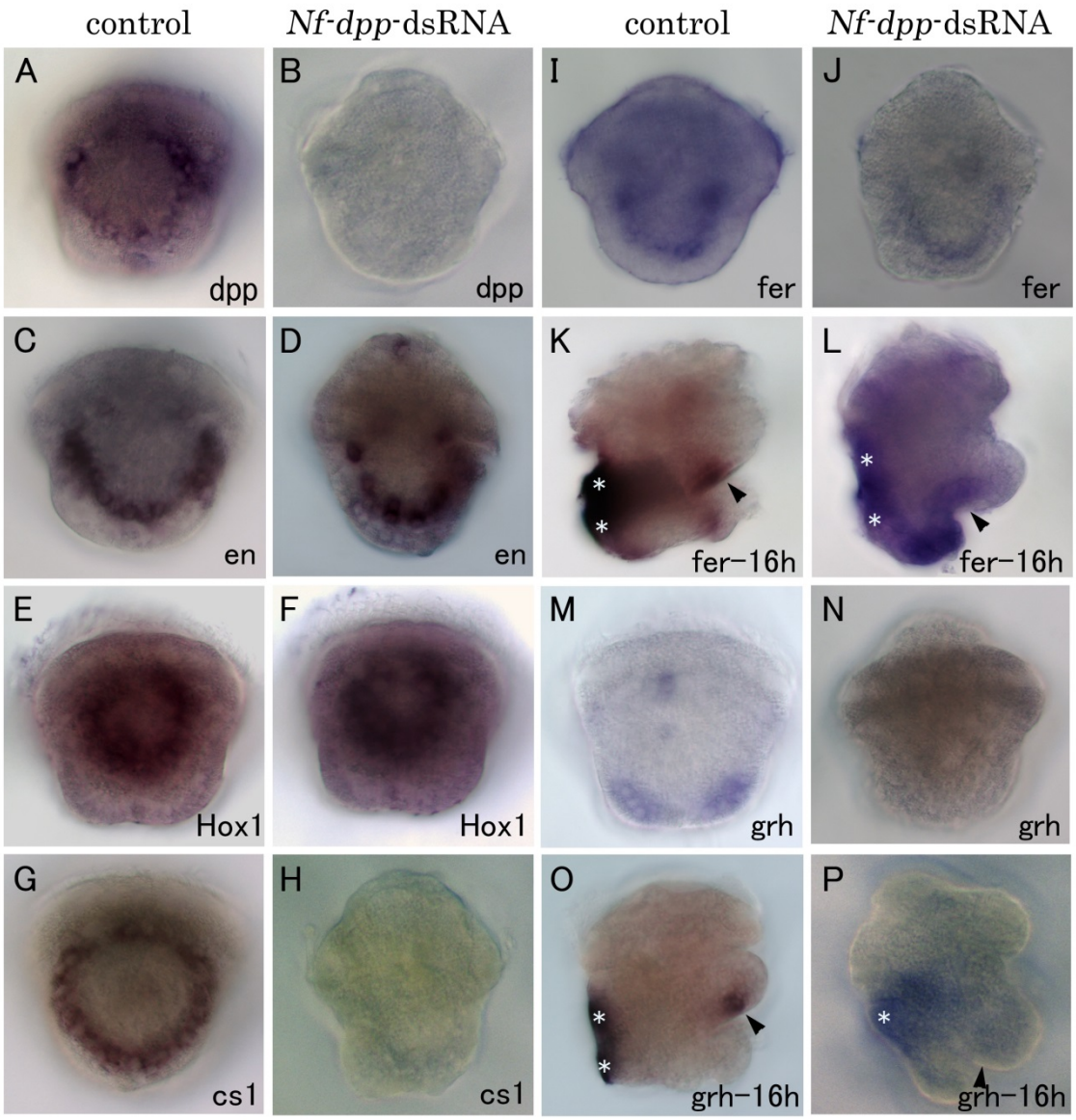
control
Nf-dpp-dsRNA
control
Nf-dpp-dsRNA
A
dpp
B
dpp
I
fer
J
fer
C
en
D
en
K
fer−16h
L
fer−16h
E
Hox1
F
Hox1
M
grh
N
grh
G
cs1
H
cs1
O
grh−16h
P
grh−16h

Fig. 6. Cleavage pattern of X blastomere and effect of sperm extracts.

(A) Summary of cleavage pattern of X (2d) lineage. Arrows indicate the cleavage order. Modified after Kurita et al. (2009). (B,C) Two-cell stage embryo before (B) and after sperm extract treatment (C). (D,E) Four-cell stage embryo before (D) and after sperm extract treatment (E). Scale bars: 50μm.

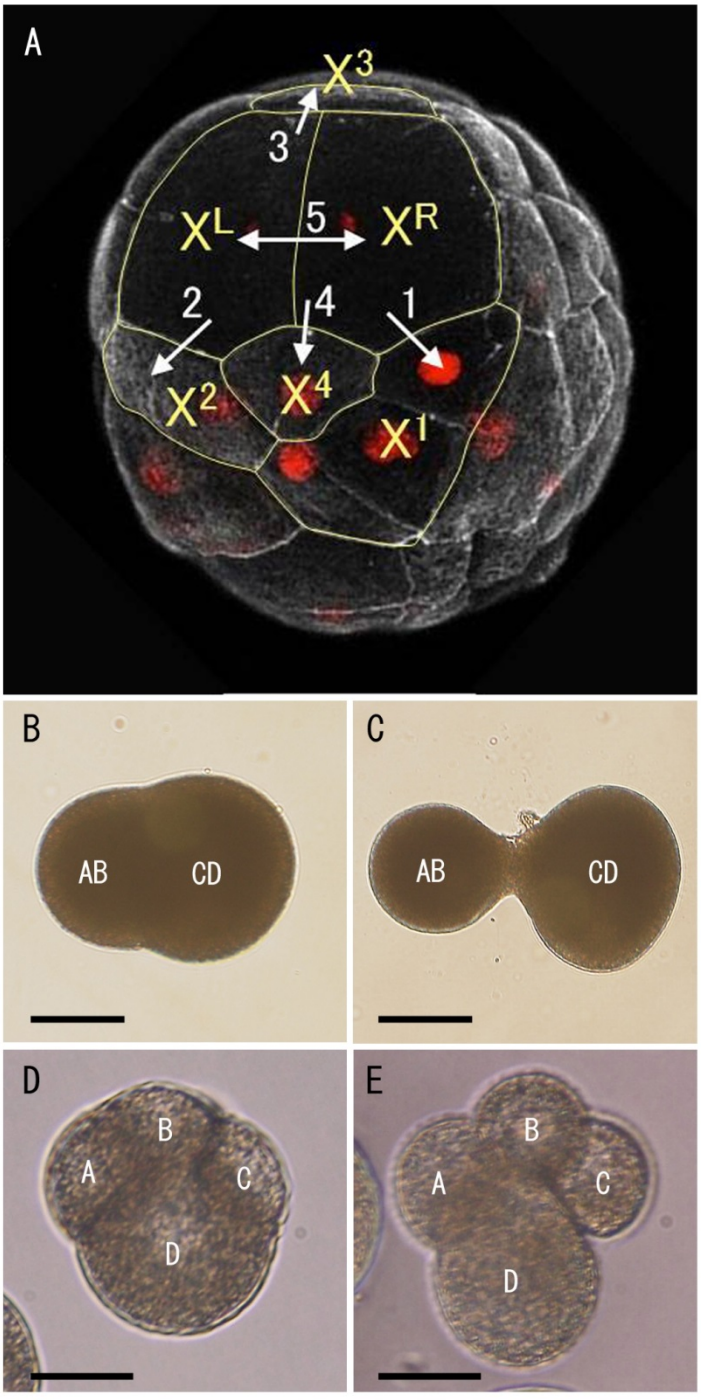
A
X3
3
XL
5
XR
2
4
1
X2
X4
X1
B
AB
CD
C
AB
CD
D
B
A
C
D
E
B
A
C
D

Fig. 7. Cleavage patterns of blastomeres isolated at the two-cell stage

(A) Isolated CD blastomeres showed unequal cleavage with polar lobes (arrowheads). (B) Isolated AB blastomeres divided symmetrically. Upper and lower panels show the time course of cleavage of blastomeres isolated from a single fertilized egg (upper and lower panel show similar stages after fertilization). Movie 1 corresponds to these figures. Scale bars: 50 μm.

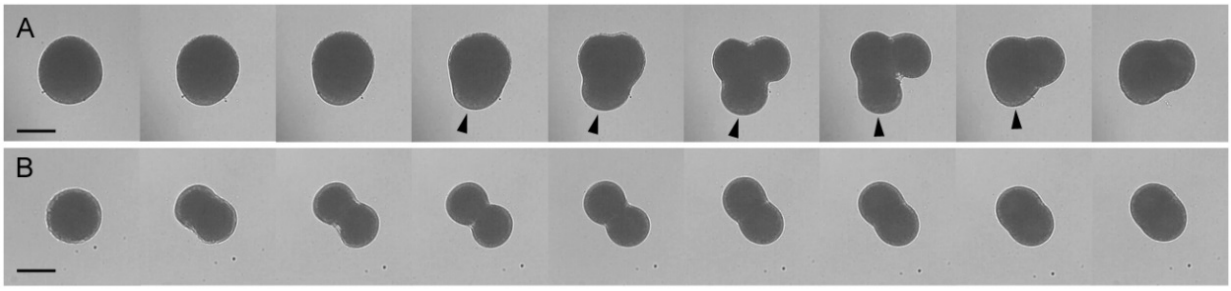
A
B

Fig. 8. Morphology of larvae developed from isolated blastomeres at 24 hpf.

(A, B) Larvae showing normal development. (C, D) Larvae developed from isolated AB blastomeres. (E, F) Larvae developed from isolated CD blastomeres. (G, H) Larvae developed from isolated D blastomeres. (A, C, E, G) Light image of the larvae. (B, D, F, H) Ciliary structures visualized using anti-β-tubulin antibody of the larvae (ventral to the left). Arrowhead: apical tuft, f: foot, broken line: mantle edge. Scale bars: 50μm

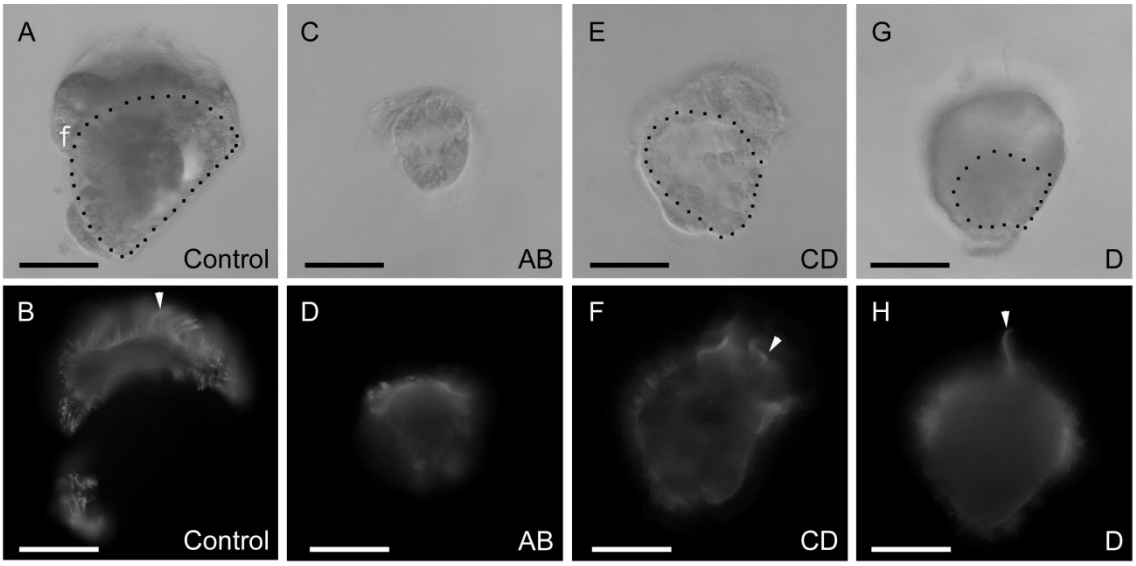
A
f
Control
C
AB
E
CD
G
D
B
Control
D
AB
F
CD
H
D

Fig. 9. Cleavage pattern of isolated D blastomere.

(A) Isolated D blastomeres after two rounds of cell divisions. (B, C) X (2d) divided unequally and smaller X^1 ($2d^2$) (B) and X^2 ($2d^{12}$) (C) localized on the same side as 2D. (D) 2D and $1d^2$ blastomeres divided, and the third division of X ($2d^{11}$) started. (E) X^3 ($2d^{111}$) was localized on the opposite side of X^1 ($2d^2$) and X^2 ($2d^{12}$). (F) After X^4 ($2d^{1122}$) divided on the opposite side of X^3 ($2d^{111}$), X ($2d^{1121}$) divided bilaterally. The broken line shows the lineage of X (2d) blastomeres. Movie 2 corresponds to these figures. Scale bars: 50 μm

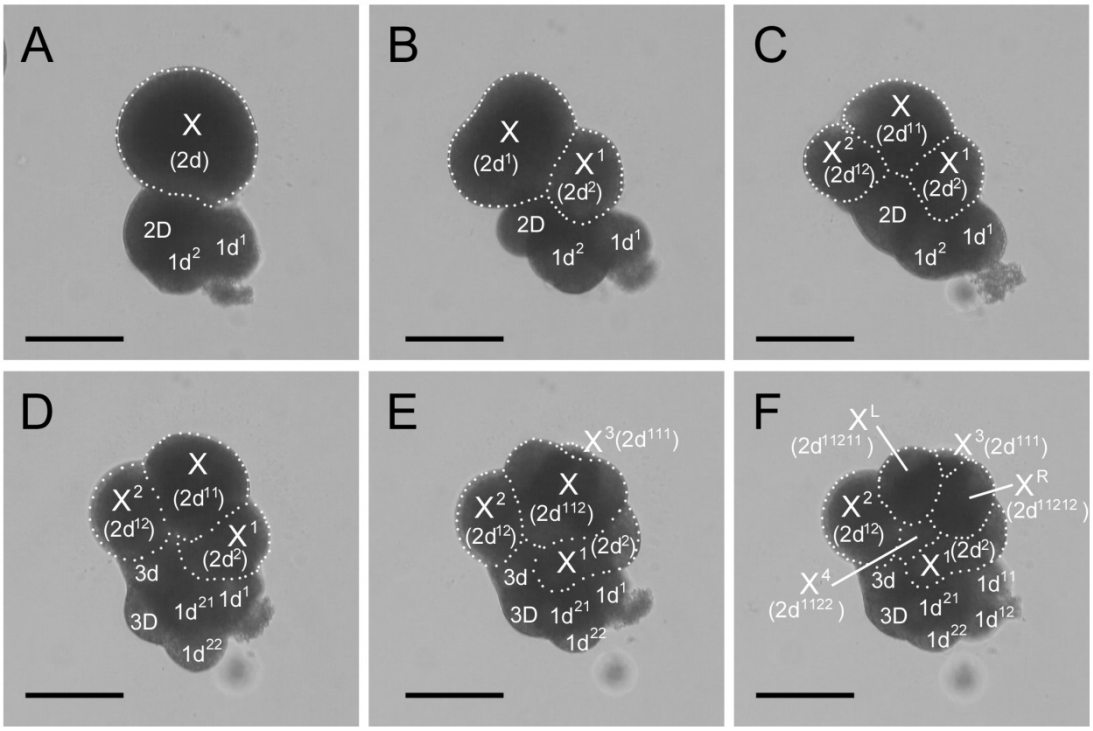
A
X
(2d)
2D
1d2
1d1
B
X
(2d1)
X1
(2d2)
2D
1d2
1d1
C
X
(2d11)
X2
(2d12)
X1
(2d2)
2D
1d2
1d1
D
X
(2d11)
X2
(2d12)
X1
(2d2)
3d
3D
1d21
1d1
1d22
E
X3(2d111)
X
(2d112)
X2
(2d12)
X1(2d2)
3d
3D
1d21
1d1
1d22
F
XL
(2d11211)
X3(2d111)
XR
(2d11212)
X2
(2d12)
X1(2d2)
X4
(2d1122)
3d
3D
1d21
1d11
1d12
1d22

Fig. 10. Expression patterns of *Sv-CS1* during normal development.

(A–C) 10 hpf larvae. (D–F) 14 hpf larvae. (G–I) 16 hpf larvae. (J–L) 24 hpf larvae. (A, D, G, J) Dorsal view of larvae. (B, E, H, K) Lateral view and focus on the mid line (ligament) of larvae (ventral to the left). (C, F, I, L) Lateral view and focus on the left surface of larvae (ventral to the left). Arrowhead: invagination site. Broken line: shell field. Scale bars: 50μm.

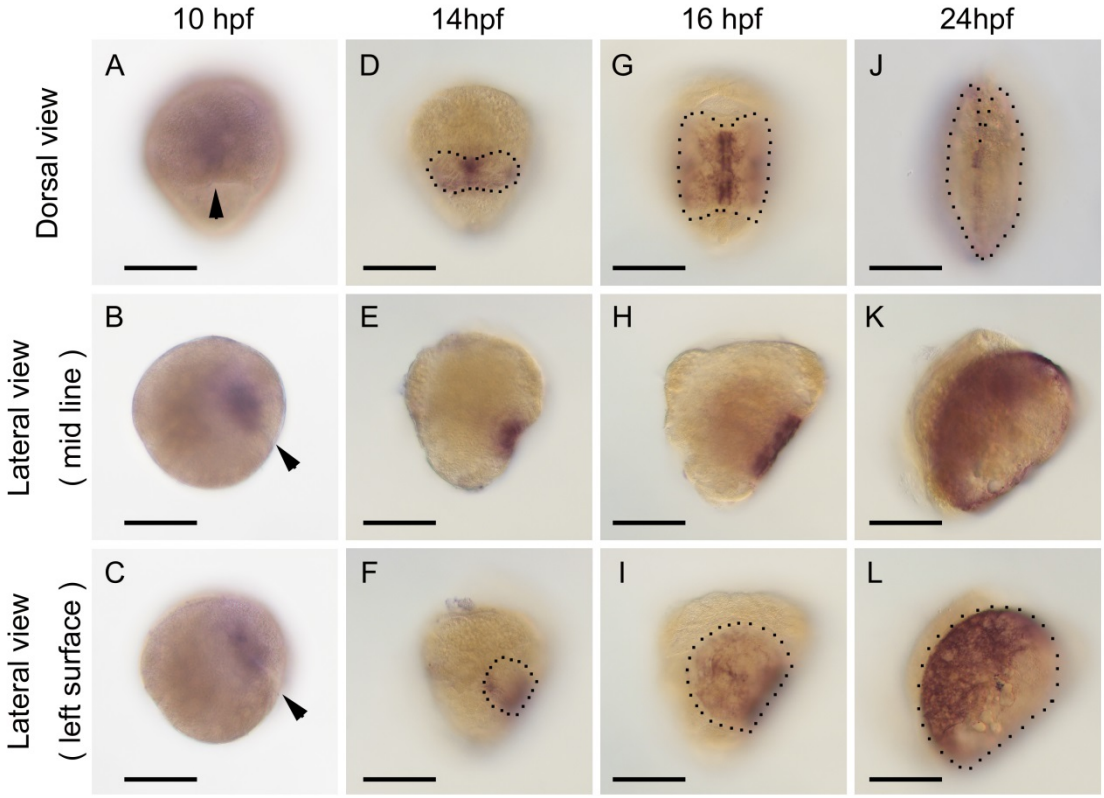
10 hpf
14hpf
16 hpf
24hpf
Dorsal view
Lateral view (mid line)
Lateral view (left surface)
A
B
C
D
E
F
G
H
I
J
K
L

Fig. 11. Expression patterns of *Sv-CS1* in larvae developed from isolated blastomeres.

(A,B) Larva developed from AB blastomeres at 24 hpf. (C–H) Larva developed from D blastomeres at 24 hpf. (A, C, E, G) Dorsal view. (B, D, F, H) Lateral view (ventral to the left). Broken line shows the shell field edge. Scale bars: 50μm.

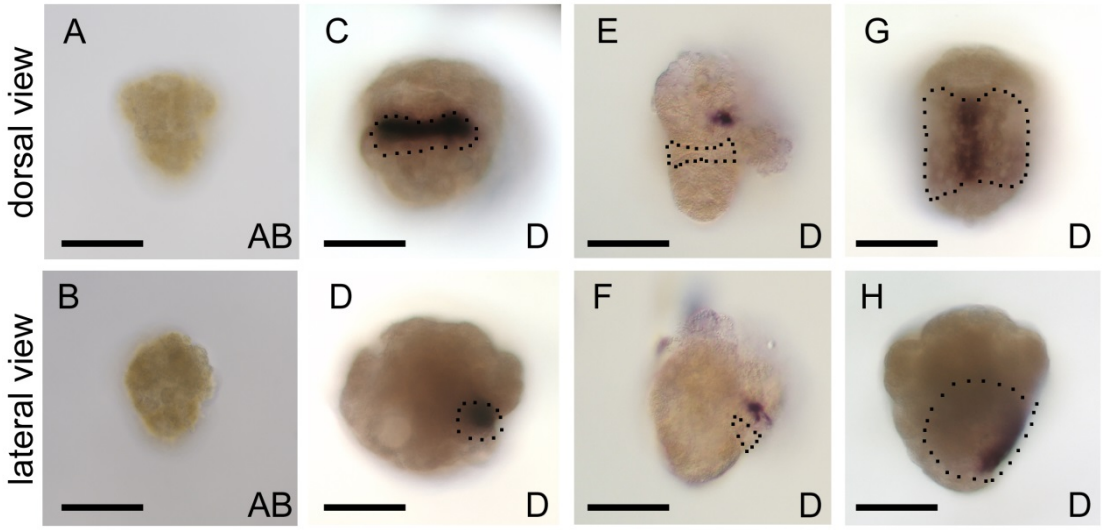
dorsal view
lateral view
A
B
C
D
E
F
G
H
AB
AB
D
D
D
D
D
D

Movies and Legends

Movie 1. Cleavage pattern of blastomeres isolated at the 2-cell stage from a single fertilized egg after sperm extract treatment.

Left is CD blastomere and right one is AB. Fig. 7 corresponds to this movie.

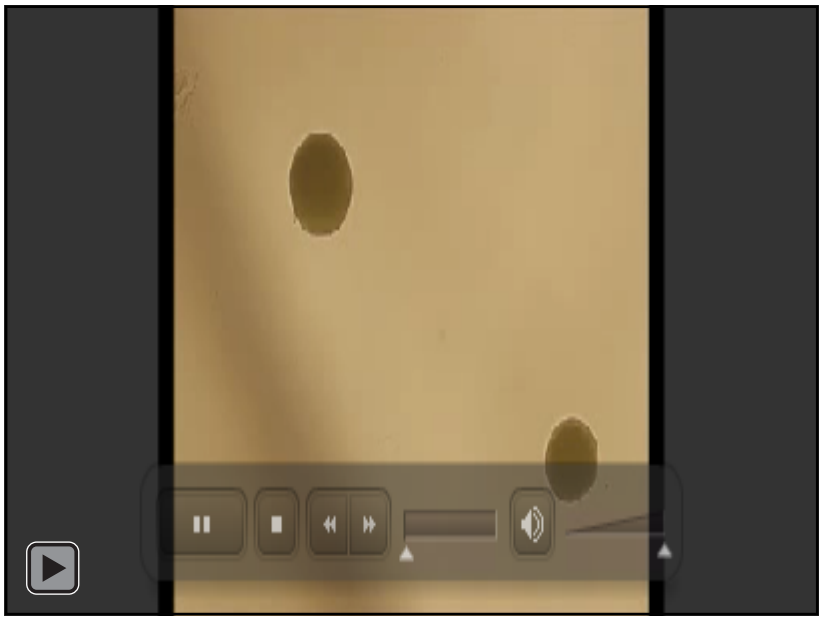

Movie 2. Cleavage pattern of isolated D blastomere after sperm extract treatment.

The dashed line shows the lineage of X blastomeres. Fig. 9 corresponds to this movie.

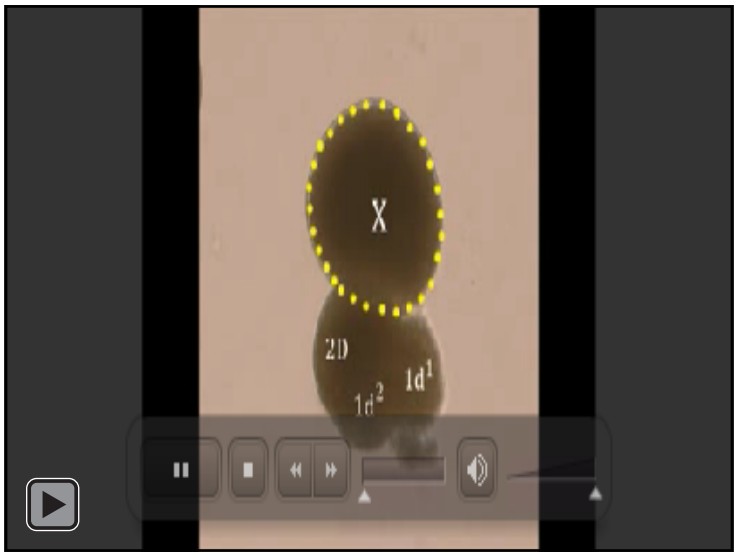
X
2D
1d2
1d1